Wang, Yuchen; Jöns, Klaus D.; Sun, Zhipei

Integrated photon-pair sources with nonlinear optics

Published in:
APPLIED PHYSICS REVIEWS

DOI:
10.1063/5.0030258

Published: 01/03/2021

Document Version
Peer reviewed version

Please cite the original version:
Wang, Y., Jöns, K. D., & Sun, Z. (2021). Integrated photon-pair sources with nonlinear optics. *APPLIED PHYSICS REVIEWS*, *8*(1), [011314]. https://doi.org/10.1063/5.0030258

Integrated Photon-Pair Sources with Nonlinear Optics

Yuchen Wang,[1, a)] Klaus D. Jöns,[2] and Zhipei Sun[1, 3, b)]
[1)]*Department of Electronics and Nanoengineering, Aalto University, Espoo, Finland*
[2)]*Department of Physics, Paderborn University, Paderborn, Germany*
[3)]*QTF Centre of Excellence, Department of Applied Physics, Aalto University, Espoo, Finland*

(Dated: 6 January 2021)

Assisted by the rapid development of photonic integrated circuits, scalable and versatile chip-based quantum light sources with nonlinear optics are increasingly tangible for real-world applications. In this review, we introduce the basic concepts behind parametric photon pair sources and discuss the current state-of-the-art photon pair generation in detail bur also highlight future perspectives in hybrid integration, novel waveguide structures and on-chip multiplexing. The advances in near-deterministic integrated photon pair sources are deemed to pave the way for the realization of large-scale quantum photonic integrated circuits for applications including quantum telecommunication, quantum sensing, quantum metrology and photonic quantum computing.

I. INTRODUCTION

Integrated quantum photonics arises from the encounter of two fields that have revolutionized our understanding of the nature and are starting to reshape our future: quantum technology and integrated photonics.[1–3]

Quantum technology, which enables us to generate, manipulate and detect quantum states in a complex system, has attracted increasing attention in recent years[4]. Its applications including metrology[5], computing[6,7], sensing[8,9] and communication[10] are deemed to change the way in which we measure, process, and transmit and store information. Many proof-of-principle experiments of quantum information science employing single-photons have been demonstrated with free-space optics. The integration and miniaturization of such systems independent of laboratory environment will be crucial for large-scale implementations and real-world applications[11–13].

Integrated photonics, and in particular silicon photonics, has been considered one of the most suitable platforms for next-generation data processing and telecommunication applications[14,15]. Being compatible with the current mature electronic integrated circuit manufacturing infrastructure, it is inherently cost- and power-efficient. In recent years, quantum photonic integrated circuits (QPICs) were experimentally demonstrated on the silicon photonic platform[16]. Other material platforms such as silicon nitride (SiN), lithium niobate (LN), III-V semiconductors and fiber devices are also being actively investigated for QPIC applications[12,17].

To implement a quantum photonic integrated circuit (QPIC) with practical functionalities, fundamental building blocks for the generation, manipulation and detection of quantum states of light are in immediate need of development[2]. Tremendous efforts have been devoted to the study of efficient generation of single-photons and correlated photon pairs[18]. For their simplicity of implementation with integrated photonic devices, the photon pair source exploiting nonlinear frequency conversion processes is a promising alternative to the atom-like single-photon emitter. By optimizing nonlinear light-matter interaction with quasi phase-matching techniques or passive enhancement of electric field in resonant structures, high-brightness photon pair sources have been developed providing heralded single-photons with high degrees of indistinguishability. Various techniques have been employed to directly generate two-photon and multi-photon entangled states on integrated photonic chips via nonlinear processes that can be directly applied for on-chip quantum information processing or computing[19,20].

In this article, we review recent advances of integrated photon pair sources with nonlinear optics. In Section II we describe the basic concepts of photon pair generation via nonlinear parametric processes, the main parameters for photon pair source characterization and the most promising integration material platforms. The current state-of-the-art high-efficiency generation of both heralded single-photons and entangled states is discussed in Section III. Future perspectives of integrated photon-pair sources are discussed in Section IV. A short conclusion is given in Section V.

II. FUNDAMENTALS OF PHOTON PAIR GENERATION WITH NONLINEAR OPTICS

Nonlinear optics has been intensely studied and now deeply involved in many photonic applications, in particular, the generation of coherent electromagnetic waves through nonlinear parametric processes[21], such as second harmonic generation (SHG), four-wave mixing, and difference frequency generation. The generation of quantum-correlated pairs of photons is based on spontaneous parametric processes such as spontaneous parametric down-conversion (SPDC) and spontaneous four-wave mixing (SFWM) arising from $\chi^{(2)}$ or $\chi^{(3)}$ nonlinearities of materials, respectively[22]. In SPDC and SFWM processes, pump photons generate pairs of signal and idler photons probabilistically. The detection of one photon of the pair could herald the presence of the other since they are inherently correlated in time and energy.

[a)]Electronic mail: yuchen.1.wang@aalto.fi
[b)]Electronic mail: zhipei.sun@aalto.fi

A. Nonlinear processes for photon-pair generation

The optical parametric nonlinearity of a material is often described by the Taylor expansion of its electric susceptibility χ_e. The instantaneous response of the dielectric polarizability density $\mathbf{P}(t)$ of an optical medium to an external electric field $\mathbf{E}(t)$ can be written in a vectorial form as[21]:

$$\mathbf{P} = \mathbf{P}^{(1)} + \mathbf{P}^{(2)} + \mathbf{P}^{(3)} \dots \quad (1)$$

$$= \varepsilon_0(\chi^{(1)}\mathbf{E} + \chi^{(2)}\mathbf{E}^2 + \chi^{(3)}\mathbf{E}^3 + \dots), \quad (2)$$

where ε_0 is the vacuum electric permittivity; $\mathbf{P}^{(i)}$ and $\chi^{(i)}$ are the i$^{\text{th}}$-order polarization and susceptibility, respectively. This vectorial expression can be written in a scalar form using a Cartesian basis and expressing susceptibilities as tensors. The second- and thrid-order polarization can be written as:

$$P^{(2)} = \varepsilon_0 \sum_{jk} \chi^{(2)}_{ijk} E_j E_k \quad (3)$$

$$P^{(3)} = \varepsilon_0 \sum_{jkl} \chi^{(3)}_{ijkl} E_j E_k E_l, \quad (4)$$

where the indices i, j, k and l are the corresponding x, y and z components of the interacting electric field.

Conventionally, the second-order nonlinearity of an optical material is often characterized by its contracted second-order susceptibility tensor d_{il} of the full tensor $d_{ijk} = \chi^{(2)}_{ijk}/2$, when the condition of Kleinmann symmetry is satisfied[21]. Instead, the third-order nonlinearity of an optical material is often charactrized by the nonlinear refractive index n_2:

$$n_2 = \frac{3}{4n_0^2 c\varepsilon_0}\chi^{(3)}, \quad (5)$$

Traditionally, in free-space propagation the nonlinear interaction is optimized by a proper orientation of a birefringent nonlinear crystal for achieving the phase-matching condition between the interacting wave components, due to the limitation that most commonly used nonlinear material exhibit normal dispersion in visible to near-infrared wavelength range[21]. However, with the possibility of dispersion engineering, optical waveguides can permit the phase-matching condition to be satisfied with a broader bandwidth, e.g. the full width at half maximum gain bandwidth of four-wave mixing exceeding 300 nm at telecom wavelength[23].

With the involvement of multiple wave components at different frequencies, many processes such as sum frequency generation, difference frequency generation and frequency doubling could take place if their relative conditions were satisfied. The second-order SPDC and the third-order SFWM processes generally used for photon-pair generation are discussed in detail as follows.

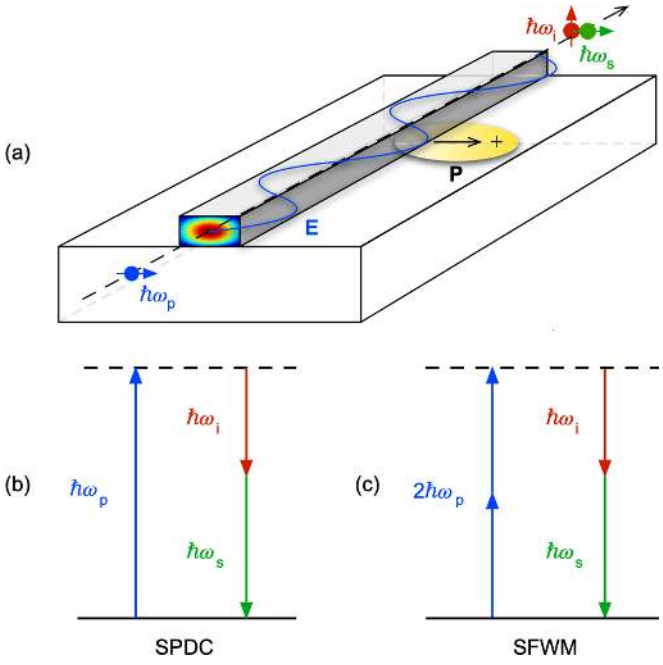

FIG. 1. The fundamentals of the nonlinear photon pair generation in integrated waveguides. (a) An illustration of polarization-entangled photon pair generation in a ridge channel waveguide via nonlinear light-matter interaction. The blue curve represents the oscillating electric field component of the guided pump light for the pair generation and the interaction dipole is represented by the golden sphere. The equivalent energy diagrams of (b) the SPDC process and (c) the SFWM process with degenerate pump, where the dashed line represents the virtual excited state. **E**, instantaneous electric field. **P**, field-induced dipole oscillation. $\hbar\omega_{p,s,i}$, photon energies of pump, signal and idler.

1. *Spontaneous parametric down-conversion*

If a crystalline material is non-centrosymmetric, its electronic potential function is asymmetric. This leads to non-zero even order susceptibilities, including the second-order term $\chi^{(2)}$. In such a nonlinear material, various second-order nonlinear optical frequency mixing processes involving three wave components can take place when both energy and momentum conservation conditions are satisfied, such as SHG and SPDC.

The SPDC process is typically illustrated as an electron being excited by a pump photon to a virtual level corresponding to $\hbar\omega_p$ and then decays by spontaneously emitting two photons referred to as the signal and the idler (here we simply define the wave component with lower frequency as 'idler' and the other as 'signal'; they do not share the traditional denotation as in a parametric amplification process where the amplified wave is referred to as the signal), whose sum in frequency equals to that of the pump $\omega_s + \omega_s = \omega_p$, as shown in Fig.1(b). Here we consider the most commonly used degenerate case in which the signal and idler are both at half of the pump's frequency $\omega_{s,i} = 1/2\omega_p$. The energy and momentum conservation laws during this process require that:

$$\hbar\omega_{\mathrm{p}} = \hbar\omega_s + \hbar\omega_i, \tag{6}$$

$$\Delta k = k_s + k_i - k_p \approx 0, \tag{7}$$

where Δk represents the phase mismatch in the nonlinear process, $\hbar$ is the Plank constant and $k_{p,s,i}$ are magnitudes of the wave vectors of the pump, signal and idler waves.

The SPDC process could be considered as an inverse sum-frequency generation (non-degenerate) or an inverse SHG process (degenerate). With a detailed quantum treatment of the SPDC process, it can be shown that the process is probabilistic in which an arbitrary quantity n of photon pairs can be generated ($n = 0, 1, 2, \dots$) each with an associated probability. The pair generation rate (PGR), which indicates the number of photon pairs generated per second (with a unit of s^{-1} or Hz), can be shown to have the following dependence[24–26]:

$$r_{\mathrm{SPDC}} \propto \frac{4{d_{\mathrm{eff}}}^2 P_{\mathrm{p}} L^2}{9\varepsilon_0^2 c^2 A_{\mathrm{eff}}} \mathrm{sinc}^2\left(\frac{\Delta k L}{2}\right), \tag{8}$$

where r_{SPDC} is the PGR for the SPDC process, P_{p} is the pump power, A_{eff} is the mode interaction overlap area and in a waveguide this can be approximated by the effective mode area of the smaller mode among the wave components, L is the waveguide length and d_{eff} is the effective value of the second-order nonlinearity tensor. The sinc term takes into account the non-perfect phase-matching among the wave components, limiting the useful waveguide length to around the coherence length $L_{\mathrm{c}} = (2/\Delta k)$. From this expression, we can conclude that increasing the light confinement contributes inverse-linearly to the PGR. An increasing pump power instead contributes only linearly to the PGR in the SPDC process[24]. At the same time, if the phase mismatch is small enough, increasing the length of the waveguide would also quadratically increase the rate of pair generation.

2. Spontaneous four-wave mixing

The SFWM is a third order nonlinear process and involves four wave components. In a degenerate pumping scheme, two pump photons at ω_{p} generates a pair of photons at ω_{s} and ω_{i} around ω_{p}. It can be typically illustrated as shown in Fig.1(c), in which an electron is excited by two pump photons to a virtual level corresponding to $2\hbar\omega_{\mathrm{p}}$ and then decays by emitting two photons with energy $\hbar\omega_{\mathrm{s}}$ and $\hbar\omega_{\mathrm{i}}$. The energy and momentum conservation laws during this process require:

$$2\hbar\omega_{\mathrm{p}} = \hbar\omega_{\mathrm{s}} + \hbar\omega_{\mathrm{i}}, \tag{9}$$

$$\Delta k = k_s + k_i - 2k_p \approx 0, \tag{10}$$

Under more detailed treatments of the FWM process, the phase-matching condition will also include an additional phase term accounting for the nonlinear phase accumulation related to the Kerr effect, the free carrier effect and the Raman scattering[23,27]. As in many cases the four interacting wave components have very small differences in frequency, the phase matching condition can be easily satisfied with a proper dispersion engineering of the integrated waveguide structure.

An associated photon-pair generation rate can be written also for the SFWM process, assuming a near-perfect phase matching[28,29]:

$$r_{\mathrm{SFWM}} \propto \left|\frac{3\omega_{\mathrm{p}}\chi^{(3)}}{2n_0^2\varepsilon_0 c^2 A_{\mathrm{eff}}} P_{\mathrm{p}} L\right|^2 = \left|\frac{2\omega_{\mathrm{p}} n_2}{c A_{\mathrm{eff}}} P_{\mathrm{p}} L\right|^2, \tag{11}$$

where A_{eff} is the mode interaction overlap area, ω_{p} is the pump wavelength, n_2 is the nonlinear refractive index of the waveguide material, c is the speed of light and n_0 is the refractive index at the pump wavelength. This expression shows that, under the assumption of a near-perfect phase matching, the generation efficiency of photon pairs via SFWM depends quadratically on the material nonlinearity, the pump power and the inverse of the mode size. Similar to the SPDC process, the PGR depends again quadratically on the waveguide length L in the SFWM process.

Considering the guided-wave nature of PICs, the effective third order nonlinearity of a waveguide structure can be described by the nonlinear coefficient $\gamma\,[\mathrm{m}^{-1}\mathrm{W}^{-1}]$ defined as[15]:

$$\gamma = \frac{\omega_{\mathrm{p}} n_2}{c n_{\mathrm{eff}}}, \tag{12}$$

The nonlinear coefficient γ takes into account both the material nonlinearity and the mode confinement of the waveguide.

3. Differences between SPDC and SFWM

SFWM and SPDC can both be employed for photon pair generation and they share some common grounds in the optimization of the pair generation rate. For example, in waveguide-based nonlinear devices, for materials with higher refractive index such as silicon and gallium arsenide, the mode confinement could be stronger when the cladding has a much lower index (e.g. silicon oxide or air) hence increasing light intensity and enhancing the nonlinear conversion efficiency.

There are some significant differences that limit their compatibility with different material platforms. First of all, SPDC requires that the nonlinear medium shows second-order nonlinearity, either naturally in non-centrosymmetric crystals or induced by strain[30] and photo-galvanic effect[31] or by tuning the structure orientation of 2D crystals[32]. As a result, SFWM is more widely applicable, since all materials exhibit odd order nonlinearities. Secondly, the phase matching condition for SPDC is more restrictive as the pump and the generated pair are separated in wavelength by a factor of two. The SPDC

therefore requires special strategies to be typically used such as exploiting quasi-phase-matching in periodic structures[33] or Bragg reflection waveguides[34].

B. Material platforms for nonlinear integrated photonics

Several material platforms used for integrated nonlinear optics are being considered for QPIC implementations. The essential requirements of a potential material platform for the generation of photon pairs via nonlinear parametric processes typically include high $\chi^{(2)}$ and $\chi^{(3)}$ nonlinearities, low linear and nonlinear losses (e.g. due to two-photon absorption and free-carrier absorption) losses within desired wavelength ranges, availability of appropriate integrated pump sources and the availability of mature manufacturing processes. As an example, for quantum communication, the compatibility with current telecom infrastructure is of great importance. Therefore, one of the focuses of the photon pair source development is to achieve high performance at around 1.55 μm. Mature manufacturing processes and low losses are also crucial as complex structures are needed for integration of quantum light sources for practical applications which typically require multiple active and passive components. As an example, the preparation of entangled bi-photon states makes use of multiple directional couplers and phase shifters for on-chip path, time-bin/energy-time or polarization entanglement schemes[35–38]. Key optical properties of major materials for QPIC implementation are listed in Table I.

1. Silicon

Silicon-based platforms, in particular silicon-on-insulator (SOI), are among the most mature for PIC realization. Since the beginning of its development from 1985[39], SOI technology has been behind many recent breakthroughs in integrated photonics[40]. Following the successful demonstration of critical integrated components such as modulators, directional couplers, wavelength multiplexers and photodetectors, silicon PICs have been widely used for telecommunication and data-center interconnects[41].

Silicon is transparent from $\sim$ 1.1 μm up to 9 μm. However in the context of SOI PIC structures, the cladding material, silicon dioxide, typically limits the transmission up to around 2 μm. At the telecom wavelength around 1.55 μm, silicon-based devices have a low linear loss but a high nonlinear loss for its high TPA coefficient which limits its nonlinear figure-of-merit to less than 0.5[42]. Crystalline silicon has a centrosymmetric diamond cubic lattice. Therefore, silicon crystal lacks intrinsic $\chi^{(2)}$ nonlinearity which makes it unsuited for the SPDC process. In recent years, strained silicon was demonstrated to manifest electro-optic effect and can be used for second harmonic generation[30,43]. Therefore, in principle the strain or other approaches including photogalvanic effect can be used for symmetry-breaking to enable pair generation via SPDC. On the other hand, silicon has strong $\chi^{(3)}$ nonlinearity ($n_2 = 4.5 \times 10^{-18}$ m^2W^{-1} at 1.55 μm[44]). Combined with the possibility of tight mode confinement allowed by the large refractive index contrast with respect to the most common cladding material silicon dioxide ($\Delta n \approx 2$ at 1.55 μm), silicon waveguides could provide an extremely high nonlinear coefficient γ, greater than 300 $W^{-1}m^{-1}$ at 1550 nm[45], making it a promising candidate for integrated SFWM photon pair sources.

2. Silicon nitride

Silicon nitride (typically Si_3N_4, SiN) has been routinely used in fabrication processes and final device structures for electronic integrated circuits. Following investigations of SiN waveguide structures in the 1980s, technologies for plasma-enhanced chemical vapor deposition (PECVD) and low-pressure chemical vapor deposition (LPCVD) of high-quality SiN layers have been extensively studied[46]. Recent progress on advanced SiN fabrication processes has enabled ultra-low propagation losses in waveguide structures that leads to microresonators with quality factors (Q-factor) over 10^7.[47,48] With a larger energy bandgap, SiN also shows negligible TPA in the telecom bands. A complete toolbox of high-performance PIC components including directional couplers, modulators[49,50], high-Q microresonators[47] and photodetectors[51] are also available for complex system integration, which are beneficial for fully integrated quantum photonics.

CVD SiN in the CMOS process is amorphous therefore centrosymmetric and does not exhibit $\chi^{(2)}$ nonlinearity. As a result, pristine SiN is not suited for photon-pair generation via SPDC, leaving SFWM to be the main solution for photon pair generation. Although SiN lacks second-order nonlinearity for electro-optic effects, the Kerr effect could be exploited for optical modulation[50]. On the other hand, SiN shows $\chi^{(3)}$ nonlinearity with a Kerr coefficient of $n_2 \approx 2.6 \times 10^{-19}$ m^2W^{-1} at $\sim$1.55 μm[46], more than an order of magnitude lower than that of silicon. LPCVD SiN has a refractive index of ~ 2 at 1.55 μm ($\sim$1.83 for PECVD SiN), which implies a lower index contrast compared to silicon waveguides, leading to weaker mode confinement and lower effective nonlinear coefficient. However, for its lower linear loss and the absence of two-photon absorption (TPA), SiN nonlinear waveguides can be operated at much higher power levels, in particular in the visible and telecom windows. With a combination of great linear and nonlinear optical properties, SiN is a potential alternative material platform to SOI for QPIC implementation.

3. III-V semiconductors

Among the several common semiconductor materials formed between group III elements (B, Al, Ga, In) and group V elements (N, P, As, Sb), GaAs is among the most extensively investigated and developed[63] for nonlinear optics.

GaAs is transparent from 1 to 10 μm. Waveguides in GaAs with lower than 1 dB/cm propagation loss have been demonstrated[55]. With a high refractive index of 3.4 at 1.5

TABLE I. Related properties of common materials for integrated photon pair sources. Values are at 1.55 μm if not specified. The nonlinear susceptibilities, $d_{\max}$, are the largest reported values for the corresponding orientation. The waveguide losses are the lowest values reported in the literature.

Material	n	$d_{\max}$ [pm/V]	n_2 [m^2W^{-1}]	Transparency [μm]	Propagation loss [dB/cm]
Si	3.8	15 ($\chi^{(2)}_{xxz}$ of strained-Si)[30]	4.5×10^{-18},[52]	1.1 - 9	0.026,[53]
Si_3N_4	2	-	2.6×10^{-19},[46]	0.4 - 4	0.01,[47]
GaAs	3.4	170 (d_{36} at 1 μm)[54]	1.6×10^{-17},[52]	1.0 - 10	<1,[55]
AlN	2.1	23.2 (d_{33} at 1 μm)[56]	2.3×10^{-19},[57]	0.2 - 5	0.6,[58]
$LiNbO_3$	2.21	25.2 (d_{33} at 1 μm)[54]	9.1×10^{-20},[59]	0.5 - 4	0.6,[60]
Silica	1.44	-	2.7×10^{-20},[61]	0.2 - 2	2×10^{-6}
Hydex	1.5 - 1.9	-	1.15×10^{-19},[62]	0.2 - 2	0.06,[62]

μm, strong mode confinement can be realized. Bragg-grating reflector waveguides, phase shifters, modulators, directional couplers are readily available on GaAs platform thanks to many years of active research in the field[63,64].

GaAs has a non-centrosymmetric crystalline structure which leads its non-zero $\chi^{(2)}$ nonlinearity. Furthermore, GaAs possess one of the highest second-order nonlinearity ($d_{36} \approx 170$ pm/V at 1 μm[27]) and a very strong Kerr coefficient $n_2 \approx 1.6\times10^{-17}$ m^2W^{-1} at 1.5 μm[52]. Therefore, both SPDC[65] and SFWM[66] processes could be used to generate photon-pairs in GaAs/AlGaAs waveguides, making it a very versatile platform. The mature laser diode technology on III-V semiconductor platform could also be exploited to build monolithic electrically injected photon-pair sources[67].

In recent years, alternative III-V semiconductors including AlN, GaN, GaP and InP were also investigated for integrated photonic devices. AlN shows optical properties similar to SiN (refractive index, transparency and n_2) but possesses second-order nonlinearity, for which it has been used for the development of ring resonators for photon pair generation via SPDC[58,68]. The III-V materials are also widely used for the development of quantum dots as single-photon and photon-pair emitters[69].

4. Lithium niobate

Lithium niobate (LN) is one of the most widely used materials for nonlinear frequency conversion[70]. LN is transparent in a wide wavelength range from 0.5 to 4 μm. Assisted by the advance in femtosecond laser micromachining technique[71], ion in-diffusion[72] or proton exchange techniques[73], ultra-low-loss waveguides (0.6 dB/cm) have been realized in LN[60]. With intrinsic birefringence and ferroelectricity, LN can be periodically poled (PPLN) with alternate domains of inverted electric dipole orientation to meet quasi phase-matching conditions for efficient parametric generation[21].

For its non-centrosymmetric structure, LN shows both $\chi^{(2)}$ and $\chi^{(3)}$ optical nonlinear responses. Therefore, both SPDC and SFWM processes can be exploited for photon-pair generation in LN. With the capability to achieve high efficiency via QPM in a periodically poled structure, its high electro-optic coefficient (d_{33} = 25 pm/V) and Kerr coefficient $n_2 = 9.1\times10^{-20}$ m^2W^{-1},[54], PPLN has been one of the most prominent materials for high efficiency nonlinear frequency conversion. In recent years, LN-on-insulator (LNOI) wafer fabrication process has been rapidly advanced, integrated photonic components, including superconducting single-photon detectors[74,75], have been further developed[76,77]. LNOI is foreseen to become a potential platform for fully integrated quantum photonics combining sources and detectors.

5. Glasses

The optical fiber based on fused silica glass is one of the most important platforms for guided-wave optics. For its excellent properties including extremely low losses between ∼0.2 to 2 μm, low dispersion and low nonlinearity, it has been the backbone of the contemporary telecom infrastructure. Due to the low Kerr coefficient of $\sim 2.0\times10^{-20}$ m^2W^{-1},[61], standard step-index fused silica fiber is not the most suitable for nonlinear optics. By engineering the fiber geometries, photonic crystal fibers (PCFs) can have greatly enhanced effective nonlinearity due to the strong field confinement and unique dispersion engineering capability. Fused silica is in an amorphous glass state therefore it is centrosymmetric and lacks second-order nonlinearity. However, poling can be applied to silica fibers to enable second-order nonlinear processes including SPDC for photon pair generation. On the other hand, SFWM could be used in standard silica fibers.

High-index glass (Hydex™) is a special type of doped fused silica glass with refractive index in the range from 1.5 to 1.9. It has been used as an alternative material for CMOS compatible low-loss optical waveguides. It has a relatively low Kerr nonlinearity of $\sim 1.15\times10^{-19}$ m^2W^{-1}, between fused silica and silicon nitride. The low nonlinearities could be mitigated by the possible high quality-factor (Q-factor) of micro-ring resonators beyond 10^6 to provide an attractive level of performance for photon pair generation[62].

Chalcogenide glasses including As_2S_3 and As_2Se_3 have also attracted considerable attention for their high nonlinearities ($n_2 \approx 3\times10^{-18}$ m^2W^{-1} for As_2S_3[78]). They have excellent transparency in the mid-IR region where conventional silica glass shows strong absorptions[79]. Chalcogenide step-index[80] and microstructured fibers[81] have been widely used for supercontinuum generation in the mid-IR region for frequency comb synthesis. Therefore, they are suited for photon pair

generation via SFWM especially in the mid-IR region.

C. Fundamentals of photon pair sources

Being a quantum light source, photon pair sources are usually characterized in ways radically different from those commonly used for traditional coherent light sources such as laser sources. In this Section, we introduce very concisely the general parameters and terminologies used for the quantitative characterization of the photon pair sources.

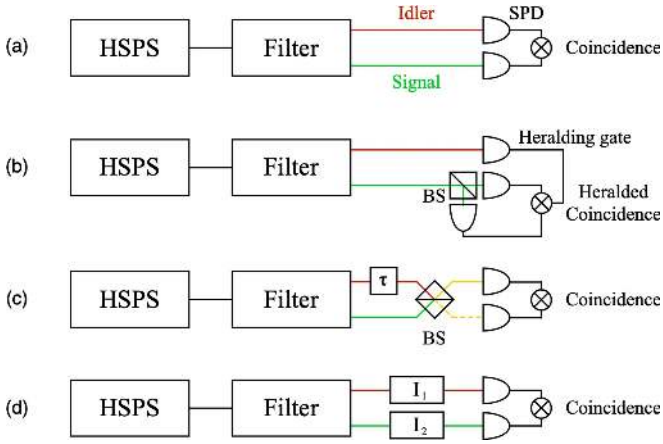

FIG. 2. Typical photon pair source characterization setups for: (a) inter-beam coincidence counting, (b) intra-beam heralded coincidence counting with an HBT interferometer, (c) TPI for indistinguishable photons in a HOM interferometer and (d) TPI for entangled photons with a Franson interferometer. HSPS, heralded single photon source. Filter, e.g. WDM to separate the signal and the idler and reject the residual pump. SPD, single photon detector. BS, 50:50 beam splitter. $I_{1,2}$, interferometers (e.g. Michelson or Mach-Zehnder interferometers) with variable delays. Note that for the degenerate SPDC process the signal and the idler are at the same frequency and could be separated with polarization optics when they are cross-polarized.

1. *Characterization of photon pair sources*

The performance of a photon pair source could be characterized by a few commonly used parameters[19,82,83] including:

• Pair generation rate (PGR, r), which is the rate of on-chip pair generation events. The pair generation rate usually refers to the inferred numbers of pairs generated per second inside the waveguide from the measured coincidence rate C divided by the efficiencies of signal collection (η_c) and single-photon detectors (η_d):

$$r = \frac{C}{\eta_{\mathrm{c}}\eta_{\mathrm{d}}}; \tag{13}$$

• Brightness (B) of the pair source, which is a normalized PGR per unit pump power P_{p} and unit spectral bandwidth $\Delta\lambda$, with a unit of Hz/mW/nm (or Hz/mW^2/nm to emphasize the quadratic dependence on pump power):

$$B = \frac{r}{P_{\mathrm{p}}\Delta\lambda}; \tag{14}$$

• Coincidence (C) and accidental (A) count rates, which are the measured rate at which coincidences of signal and idler photons, can be measured in a standard measurement configuration shown in Fig.2(a).

$$\begin{aligned} C_{raw} &= (\eta_{\mathrm{c,s}}\eta_{\mathrm{d,s}})(\eta_{\mathrm{c,i}}\eta_{\mathrm{d,i}})r + A && (15)\\ &= \eta_{\mathrm{s}}\eta_{\mathrm{i}}r + A && (16)\\ &= C_{net} + A, && (17) \end{aligned}$$

where $\eta_{\mathrm{c/d,s}}$, $\eta_{\mathrm{c/d,i}}$ and $\eta_{\mathrm{s,i}}$ are collection, detection and total efficiencies of signal and idler photon counting measurements, respectively. The net coincidence rate is the measured raw coincidence rate minus the accidental coincidence rate which includes the detector dark count rate and accidental counts due to noises in the generation processes:

• Coincidence-to-accidental ratio (CAR), which is a measure of the signal-to-noise ratio of the source and equals to the ratio between the net coincidence count rate and the accidental count rate. Consider that at the signal and idler detection branches, uncorrelated photons due to noises in the waveguides (e.g. due to spontaneous Raman scattering) and in the detectors will be counted towards the total signal. The unconditioned photon count rates of the signal and idler detectors N_s and N_i can be written as:

$$N_{s,i} = \eta_{s,i}(r + n_{s,i}) + d, \tag{18}$$

where $n_{s,i}$ are the uncorrelated noise photon generation rates for signal and idler branches and d is the dark count rate of the single photon detectors. The net CAR can be written as[84]:

$$\begin{aligned} CAR &= \frac{C_{net}}{A} && (19)\\ &= \frac{\eta_{\mathrm{s}}\eta_{\mathrm{i}}r}{N_i N_s} && (20)\\ &= \frac{\eta_{\mathrm{s}}\eta_{\mathrm{i}}r}{[\eta_s(r+n_s)+d)(\eta_i(r+n_i)+d)]}. && (21) \end{aligned}$$

To understand the general behavior of CAR, here we assume that $\eta_s \approx \eta_i$ and $r \gg n$. At low pump powers, $\eta r \ll d$, the accidental coincidence is dominated by the dark count rates of the detectors, CAR can be expressed as CAR $\approx \eta^2 r/d^2$. At high pump power, the accidental rate is dominated by the pair generation rate itself ($\eta r \gg d$), giving an expression as CAR $\approx 1/r$ (this is due to the probability of generating multiple pairs, please see Refs.[84,85]). As a result, CAR increases linearly with pump power at low power levels until a maximum is reached when the detected count rate is

close to the dark count rate of the detector, afterwards it decreases inversely with further increasing pump power due to the higher chance of generating multiple pairs.

The parameters generally used to quantitatively evaluate the quality of the quantum states of light include:

• Second-order correlation function $g^{(2)}(\tau)$, which characterizes the degree of photon anti-bunching, can be retrieved using the Hanbury Brown-Twiss (HBT) experiment by means of a heralding gate shown in Fig.2(b)[19,82]. $g^{(2)}(\tau)$ can be expressed as following:

$$g^{(2)}(\tau) = \frac{\langle I(t)I(t+\tau)\rangle}{\langle I(t)\rangle\langle I(t+\tau)\rangle}. \tag{22}$$

where I is the intensity of the light being characterized and $I(t) = c\varepsilon_0 E(t)^2/2$, the angle brackets denote the time average by integrating over a long time period. When the photons are in discrete photon number states (Fock states), the intensities $I(t)$ in the second-order correlation function can be substituted by the number of photon counts registered on the detectors at the given time $N(t)$. Theoretically, following a quantum treatment of the HBT experiment[82], the second-order correlation function at zero delay can be written as:

$$g^{(2)}(0) = 1 - \frac{1}{n}, \tag{23}$$

where n is the eigenvalue of an anti-bunched photon number state $|n\rangle$. For a ideal heralded single photon source ($n = 1$), its $g^{(2)}(0)$ approaches zero;

• Two-photon interference (TPI) effects are often used for the characterization of photon indistinguishability. With a Hong-Ou-Mandel (HOM) interferometer[86] as shown in Fig.2(c) realized with additional heralding gates, one can retrieve HOM dip visibility V_{HOM} as a measure for the indistinguishability and purity of generated photons.

• Entangled two-photon states can be characterized, for polarization entangled photon-pair sources, with a simple coincidence setup (similar to Fig.2(a)) by adding waveplates for the polarization control and polarizers as filters on each of the beam paths; and for time-bin/energy-time entangled photon-pair sources, with a Franson interferometer[87] as shown in Fig.2(d). The quality of entangled two-photon states from a photon-pair source could be tested by evaluating the violation of CHSH (Clauser-Horne-Shimony-Holt) inequality[88] as a generalization of the Bell's test. However the Franson interferometer is known to have constraints on the range of interferometer delays and loopholes in its geometry for a proper Bell-CHSH inequality test[10,89]. By changing the relative delay or the polarization orientation between the beam paths in the two detection arms (for time-bin/energy-time entangled states or polarization entangled states, respectively), relevant coincidence measurements can be performed. In the case of polarization entanglement, the inequality condition $|S| \leq 2$ can be tested. For time-bin/energy-time entanglement, a two-photon interference visibility V_{TPI} defined as the following ratio can be retrieved:

$$V_{TPI} = \frac{C_{max} - C_{min}}{C_{max}}, \tag{24}$$

where C_{max} is the maximum coincidence rate and C_{min} is the minimum coincidence rate while varying the relative delay. This visibility can be used to test for the violation of CHSH inequality ($V_{\mathrm{TPI}} \geq 96\%$[89])

• Joint spectral distribution (JSD), more specifically the joint spectral amplitudes (JSA) and intensities (JSI) between the signal and idler photons in the SPDC and SFWM processes, are of great importance for quantum information processing and quantum communication applications[90,91], where interference between two or more independent photon sources are necessary. The JSA $f(\omega_s, \omega_i)$ between the signal and the idler photons can be written as:

$$f(\omega_s, \omega_i) = \alpha(\omega_s, \omega_i)\phi(\omega_s, \omega_i), \tag{25}$$

where $\alpha(\omega_s, \omega_i)$ denotes the pump envelope function which takes into account the energy conservation and $\phi(\omega_s, \omega_i)$ is the phase-matching function which describes the momentum conservation. The JSA could be expanded according to Schmidt decomposition into a series based on temporal eigenmodes with their corresponding coefficient (with a characteristic Schmidt number)[90].

The JSD of a pair source could be characterized by a variety of techniques, including the scanning monochromator technique and the diagonal Fourier transform spectroscopy technique. For more details on this topic please see Ref.[90]. As a result, the purity of the single-photon state can be characterized using the joint spectral measurements through the retrieval of the Schmidt number. The JSD of SPDC and SFWM sources is closely related to the property of pump pulses and the phase matching condition. With the versatility of dispersion engineering by designing the geometry of the waveguide structure, the engineering of the JSD has been demonstrated for the preparation of decorrelated photon pairs with high single-photon state purity[92,93].

2. *The ideal integrated photon pair source*

In recent years, parametric photon pair generation has been demonstrated with integrated photonic devices on different material platforms with various waveguide geometries. The common goals shared among researchers for further developments include increasing the conversion efficiency and the brightness (B) of the photon pair sources while at the same time reducing the noise in the generation process thus increasing the CAR. Ideally, generated photon pairs should have a high degree of quantum correlation ($g^{(2)}(0)$ approaching zero) and should be indistinguishable (V_{HOM} approaching 100%). Considerable efforts have been devoted to on-chip direct generation of entangled two-photon and high-dimensional entangled states with high purity (V_{TPI} approaching 100%).

Ideally, when pumped with a pulsed laser source, it is desired that a single photon pair is generated per pump pulse

for practical applications. However, due to the probabilistic nature of the parametric nonlinear process, there is always a non-zero chance to generate multiple pairs[94,95]. The photon statistics of the pair generation process as two-mode squeezed vacuum follow a thermal distribution, assuming pairs to be generated in a single spatial-temporal mode[82,96]. The probability of n pairs of photons being generated in the parametric process can be expressed as:

$$p_{\text{th}}(n) = \frac{\overline{n}^n}{(\overline{n}+1)^{n+1}}, \tag{26}$$

where $\overline{n}$ is the mean number of pairs generated in a unit time interval (e.g. during the duration of a pump pulse). For $\overline{n} = 1$ and $n = 1$, this probability is 25%, which is the maximum value achievable.

Therefore, the photon per pulse generation rate is generally kept low enough to reduce the generation efficiency hence reducing $\overline{n}$, to avoid the generation of multiple pairs. Such an approach would limit the scaling of brightness by increasing the pump power. The probabilistic nature is the main drawback of the parametric photon pair sources when compared to atom-like single-photon emitters[97] whose generation process is deterministic. Tremendous efforts have been devoted to circumventing this problem with active multiplexing[98,99], which will be discussed in more detail in Section V. Ideally, with 17 independent pair sources, a near-deterministic heralded single-photon source could be realized[100].

III. CURRENT STATE-OF-THE-ART

Since the first experimental confirmation[101] of the proposed correlated twin photon concept[102], the SPDC process has been the most frequently used technique to generate correlated photon-pairs and prepare quantum states of light in bulk nonlinear crystals[24]. In this Section we review the current state-of-the-art heralded photon-pair sources on integrated photonic platforms. The major results of photon pair sources are summarized in Table II according to their material platforms and device geometries with details discussed as follows.

A. Fiber photon pair sources

Here we include also the results in fiber devices as they can be easily integrated with waveguide-based photonic systems. Being in an amorphous state, glasses used to fabricate optical fibers such as fused silica are centrosymmetric and lack even-order nonlinear responses. For this reason, SFWM has been the most investigated mechanism for photon-pair generation in conventional optical fibers.

1. Dispersion-shifted fibers

Dispersion-shifted fibers (DSF) are special optical fibers designed to shift the zero-dispersion wavelength of fused silica from 1300 nm to 1550 nm where the fiber losses are minimal. The generation of squeezed state in a 300-meter-long DSF was demonstrated in 2001 with a Sagnac loop interferometer[109]. In the same year, fiber-based SFWM correlated photon-pair source was demonstrated in 20-meter-long double-clad and quadruple-clad optical fibers with a near-zero dispersion parameter at 1.53 μm[105]. By pumping close to the fiber zero-dispersion wavelength, quantum noise correlation measurements showed a quantum noise squeezing of 1.1 dB below the shot-noise. Soon the same group demonstrated photon-pair coincidence measurements observing a PGR of 10^3 pairs/s[103] with a CAR higher than 10,[106]. The role of Raman scattering in the SFWM processes was also studied as a major contribution to the accidental coincidence signal[104,106]. By cooling the fiber to cryogenic temperatures, noises related to spontaneous Raman scattering (SpRS) were suppressed, resulting in reduced accidental coincidences, hence increasing CAR to 30,[107], and later to >100 (at a brightness of 500 kHz/mW/nm)[108].

Entangled two-photon states were soon demonstrated with DSF-based systems. The generation of polarization-entangled two-photon state via SFWM was demonstrated in a Sagnac loop interferometer setup providing a V_{TPI} larger than 90%[110] and in combination with polarization maintaining (PM) fibers with V_{TPI} greater than 93%[113] (as shown in Fig.3(a)). Time-bin entangled photon pairs were demonstrated via SFWM in a 2.5-km-long DSF, with a V_{TPI} larger than 99.3%[112]. Following these pioneering researches in fiber-based photon-pair sources, theoretical models were also developed to describe the SFWM process in fiber waveguide structures[105,212].

2. Photonic crystal fibers

PCFs have been an innovation that broadened the boundaries of fiber technologies by trapping light inside a central core (either hollow or solid) with photonic bandgap materials. It has already been widely used for high-power ultrafast pulse delivery, extreme nonlinear optics and many other applications[213].

Following the early demonstrations of photon-pair generation in DSFs, interests in PCFs for photon-pair generation arose because of their high effective nonlinear coefficients due to tight field confinement and their versatile dispersion engineering capabilities for the multiple degrees of freedom in PCF design. Correlated photon-pair generation pumped in anomalous dispersion regime was demonstrated using a 5.8-meter-long microstructured fiber in a Sagnac loop interferometer setup and analyzed in detail the role of fiber group-delay dispersion in the SFWM process[115]. Furthermore, by pumping in normal dispersion regime, far-detuned photon-pairs were generated in single-mode PCF with a high coincidence rate of 4.5 kHz in a simple single-pass setup with only 3 meters of PCF (8 kHz coincidence rate for a 6-meter-long PCF), with a maximum PGR of 6.7×10^6 pairs/s and CAR around 5[116]. In a later work, by shifting from ns-pulse pumping to ps-pulse pumping thus mitigating influence of noises due to the SpRS, with a 2-m-long PCF, PGR was increased

TABLE II. Performance comparison of common integrated photon pair sources with nonlinear optics. DSF, dispersion-shifted fiber. PCF, photonic crystal fiber. MRR, micro-ring resonator. PhCW, photonic crystal waveguide. CROW, coupled resonator optical waveguide. BRW, Bragg reflection waveguide. O-band, 1260-1360 nm. S-band, 1460-1530 nm. C-band, 1530-1565 nm. L-band, 1565-1625 nm.

Material	Waveguide geometry	Pair wavelength	Brightness [MHz mW^{-1} nm^{-1}]	CAR	V_{HOM}	Entangled states	V_{TPI}
Silica	DSF[103–110]	C-band[104,106–113],	0.5[108]	100[108]	-	polarization[110,113], time-bin[112]	99.3%[112]
	PCF[85,114–121]	Visible[85,117–120], 700-1260 nm[85,115–120], O-band[116]	0.2[117]	8[117,118]	95%[112]	path[120,122], polarization[121]	97%[121]
	Poled fiber[123–126]	C-band[123–126]	0.5 MHz/mW[123]	1200[125]	98.8%[125]	polarization[125,126]	97%[125]
Si	Channel[127–142]	S-band[138], C-band[36,128,129,131–137,139–142], L-band[138]	0.22[129,138]	673[129]	98.7%[138]	time-bin[36,135], path[132], polarization[134,141,142], transverse mode[139], high-dimension[137]	≈100%[132]
	MRR[136,143–161]	S-band[146,149], C-band[136,143–145,147,148,150–161]	640[145]	12000[157]	-	path[153,158,160], time-bin/energy-time[154–157,159,161]	98%[155]
	PhCW and CROW[162–168]	S-band[162,163], C-band[164–168]	0.13[166]	80[166]	-	time-bin[168]	74%[168]
Si_3N_4	Channel[37,169,170]	C-band[37,169,170]	0.144[170]	10[170]	-	time-bin[37]	88.4%[37]
	MRR[171–174]	Visible[174], 700-1260 nm[174], C-band[171–173]	150[171]	3780[174]	89%[172]	time-bin/energy-time[171,173,174], frequency-bin[172],	98%[171]
PPLN (LNOI)	Channel[33,38,175–190]	700-1260 nm[185,186], O-band[33,175,177,178], S-band[182,187], C-band[38,176,179–181,183,184,188,189,191], L-band[187,190], Mid-IR[185]	250[33]	67224[190]	99%[178]	polarization[38,178,180,191], path[38,177,179,182–184], time-bin/energy-time[181,188,190], high-dimension[179]	99%[178]
III-V	BRW[34,65,192–201]	S-band[34,65], C-band[192–198,200,201], L-band[199]	1.07[196]	9260[192]	89%[196]	time-bin/energy-time[192,196], polarization[65,197–199]	99%[195]
	Channel[66,202]	C-band[66,202]	-	177[202]	-	polarization[66]	-
	MRR[68,203]	S-band[203], C-band[68]	730[68]	560[68]	-	energy-time[203]	78.4%[203]
Others	Hydex[204–207], As_2S_3[78,208], Doped silica[209], a-Si:H[210,211]	Visible[209], 700-1260 nm[209], C-band[78,204–208,210], L-band[211]	3.5[206]	12[206]	-	time-bin[204], frequency-bin[205], high-dimension[205]	93%[204]

up to 10^7 pairs/s and the coincidence rate was improved to 3.2×10^5 counts/s (or a brightness of 200 kHz/mW/nm) with a CAR of 8 (as shown in Fig.3(b))[117]. With a similar setup, pumping 1.8-m-long PCF in normal dispersion regime with ps pulses, a coincidence rate of 3.8×10^4 (50 kHz/mW/nm) counts/s was demonstrated at a CAR of 8 with a narrower intrinsic bandwidth of 0.7 nm[118].

In later works, a more detailed theoretical model was developed[85] and path-entangled states were demonstrated with two PCFs generating indistinguishable photon-pairs showing four-fold coincidence with a V_{HOM} up to 95%[119] and polarization-entangled Bell states with a fidelity of 89%[122]. With a narrow-band pumping scheme, external filtering could be avoided and V_{HOM} of 77% was demonstrated[114,120]. Using PM microstructured fibers, polarization-entangled photon-pairs were also generated at a brightness of 26 kHz/mW/nm showing V_{TPI} up to 97%[121].

3. *Other fibers*

SFWM in PM step-index optical fibers has also been investigated. In few-mode PM fibers, intermodal SFWM was employed and correlated photon pair generation has been demonstrated[214,215]. Nondegenerate dual-pump SFWM was also investigated in PM fibers for photon pair generation[216,217].

The periodic poling treatment by applying strong electric field to the optical fiber was shown to enable second-order nonlinearity in fused silica glass[218]. Correlated photon-pair generation via SPDC process was observed in periodically-poled silica fiber[123,124]. Further experiments with poled fibers have demonstrated the generation of polarization-entangled two-photon states with V_{TPI} as high as 97%[125,126] (see Fig.3(c)).

Highly nonlinear fibers are a special type of optical fiber of-

ten incorporating air-holed micro-structure claddings to maximize the mode confinement hence greatly increasing its effective nonlinear coefficient[219]. Correlated photon-pair generation and polarization-entangled two-photon states via SFWM have also been demonstrated in short sections of highly nonlinear fibers, with $V_{\mathrm{TPI}} > 98\%$ at a CAR of 29[220] and an efficiency of 0.1 pair/pulse[221].

B. On-chip waveguide photon pair sources

Various waveguide structures exploiting the optical nonlinearity of the guiding materials have also been extensively studied for photon-pair generation. The scalable integration of quantum light sources is vital for the miniaturization of quantum communication systems, photonic quantum computing systems, and other applications. In this Section, recent advances in on-chip heralded single photon and entangled-state generation are reviewed according to different geometries.

1. Channel waveguides

Channel waveguides have the simplest structures among commonly used on-chip photon pair waveguide sources. They can have rib, ridge, or buried cross-section geometries and can be arranged either in simple stripes or into spirals to significantly increase the waveguide length.

In 2001, the first PPLN waveguide-based photon pair source was demonstrated[33]. With the QPM capability of PPLN and the strong mode confinement in waveguide structures, a conversion efficiency of 2×10^{-6} was demonstrated (4 orders of magnitude higher than in typical bulk nonlinear crystals) giving a very high brightness of 250 MHz/mW/nm (measured coincidence rate of 1550 Hz) at a CAR of 7[33]. Employing nondegenerate SPDC schemes, correlated photon pairs were also demonstrated[176], and further extending the wavelength of pairs into the mid-infrared (MIR) range beyond 3 μm[185]. Soon, energy-time and time-bin entangled states were demonstrated with V_{TPI} reaching 97%[175,181] and 99%[178]. Polarization entanglement[38,178,180,184,191], path entanglement[177,179,182,183,186] and high-dimensional entanglement[179] were also demonstrated in integrated PPLN waveguides. With the rapid advance in fabrication techniques (such as proton exchange and laser inscription), entangled sources with passive and active components were integrated on-chip further showcasing the potential of the PPLN QPIC platform[38,183]. Using a dielectric coating on the waveguide endfaces, resonant cavities could be realized. Singly-[187] and doubly-resonant[188,189] optical parametric oscillator (OPO) based SPDC photon pair sources have been demonstrated showing 25-fold enhancement of conversion rate reaching a pair brightness of 2.2 MHz/mW/nm. Time-bin entanglement has been demonstrated with doubly-resonant Ti-infused PPLN waveguide[188]. With recent advances in the fabrication of high-quality PPLN waveguides, a high brightness of 56 MHz/mw/nm (at a CAR over 600) with a maximum CAR of 67000 has been achieved[190].

Silicon waveguides, with their larger Kerr coefficient (200 times higher than fused silica) and tighter mode confinement (see Table I), have effective nonlinear coefficients γ five orders of magnitude higher than that of standard optical fibers[52]. Not long after photon pair generation had been demonstrated in fibers and LN waveguides, correlated photon pair generation in silicon waveguides via SFWM was proposed[222] and experimentally demonstrated in a buried silicon rectangular waveguide[133]. Thanks to the strong nonlinearity coefficient in silicon, using a waveguide only 9.11 mm in length, with pulsed pumping, a pair production rate of ~ 0.05 pair/pulse and a CAR as high as 25 were achieved. By further suppressing the SpRS and improving input and output coupling, a maximum CAR of 673 and a brightness of 0.19 MHz/mW/nm were demonstrated[129]. The high CAR at room temperature is an evidence that the limitation due to SpRS induced noises is less prominent in the crystalline silicon as compared to the silica glass. Soon after the demonstrations of the generation of correlated photon pairs, various types of entangled two-photon states in integrated silicon waveguides were demonstrated. Time-bin entangled[36,135], path-entangled[131,132,138], polarization-entangled[134,139,140] and recently high-dimension polarization-entangled[137] states were prepared on-chip (a simple waveguide design is shown in Fig.4(a)), showing V_{TPI} higher than 99%[132] (as shown in Fig.4(b)) and very high entangled Bell state fidelity of 98.9%[138].

Compared to silicon, silicon nitride has advantages in its low linear and nonlinear losses at 1.5 μm and its high transparency in VIS-NIR range, but it has lower Kerr nonlinearity and weaker mode confinement compared to Silicon (see Table I). Photon pair generation has also been demonstrated via SFWM in double-strip[170] and silicon-rich[169] SiN waveguides achieving a 144 kHz/mW/nm brightness with CAR larger than 10. Time-bin entangled photon pairs were generated in SiN double-stripe spiral channel waveguides with a V_{TPI} of 88.4%[37] (the double-stripe waveguide structure is shown in Fig.4(c)).

III-V semiconductor photon pair sources based on SPDC have been developed in channel waveguides demonstrating correlated photon pair generation[223] and frequency-bin entanglement[195] with integrated super-lattices for quasi phase-matching. Other works using BRW structures for phase-matching are discussed in the following subsection 'other waveguide structures'. SFWM-based photon pair generation was also investigated in channel waveguides made with III-V semiconductors since they also possess large Kerr coefficients. Correlated photon pairs[202] and subsequently polarization-entangled states[66] were demonstrated in dispersion engineered AlGaAs waveguides exploiting their strong third-order nonlinearity.

Correlated photon pairs were also demonstrated in channel waveguides on other material platforms, for example, via SFWM in As_2S_3 glass channel waveguides[78]. Although possessing a high nonlinearity, this chalcogenide glass material faces similar obstacles posed by SpRS noises as silica glass for achieving high CAR.

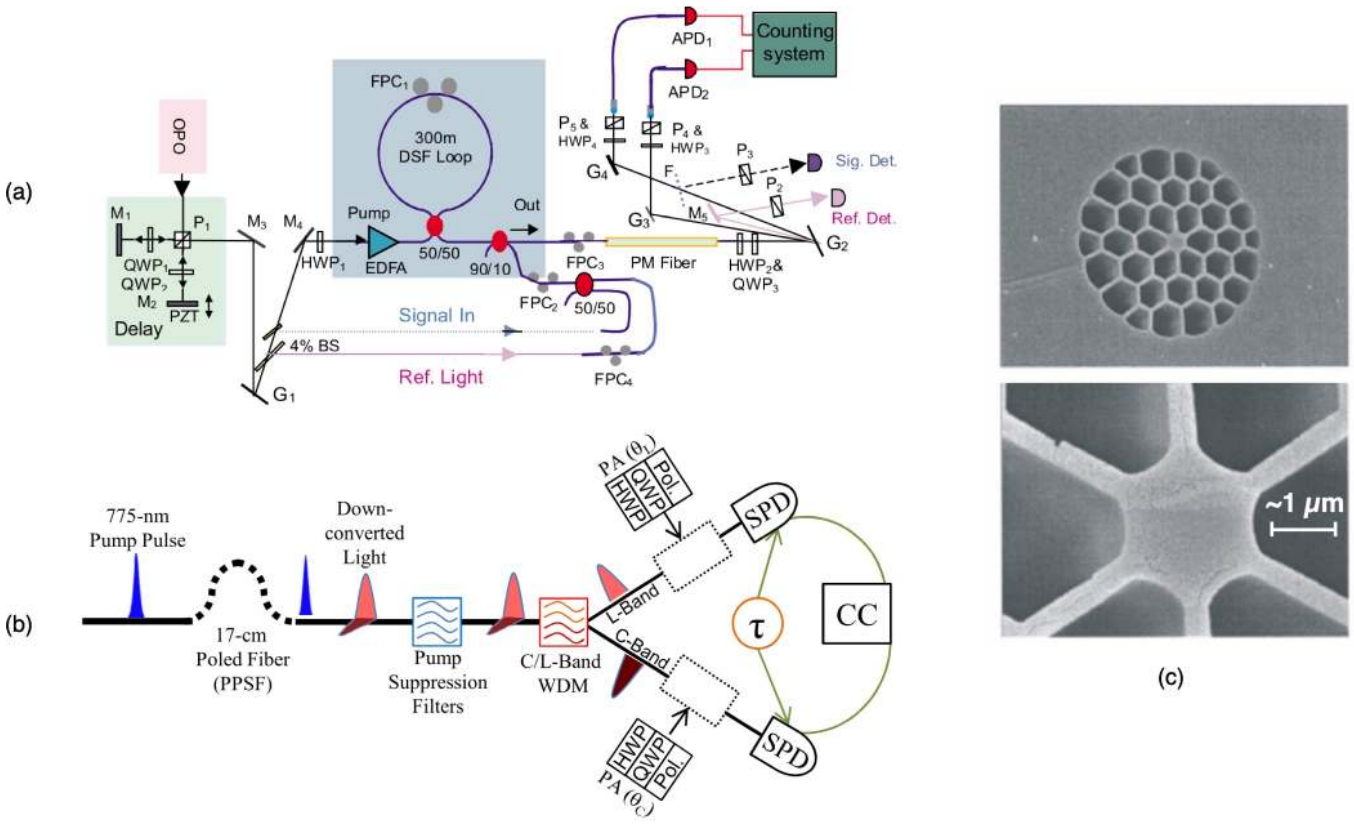

FIG. 3. Fiber-based photon pair sources. (a) Schematic illustration of an polarization-entangled photon pair source setup using the SFWM process in a Sagnac loop with a dispersion-shifted fiber (DSF). P_1-P_5, polarizing beam splitters; G_1-G_4, diffraction gratings; M_1-M_5, mirrors; FPC_1-FPC_4, fiber polarization controllers; QWP, quarter-wave plate; HWP, half-wave plate; F, flipper mirror; OPO, optical parametric oscillator; EDFA, Erbium-doped fiber amplifier; BS, beam splitter; PM, polarization maintaining; APD, avalanche photodiode. (b) Schematic illustration of an experimental setup of polarization-entangled photon pairs via SPDC in a periodically poled fiber. PPSF, periodically poled silica fiber; WDM, wavelength division multiplexer; SPD, single-photon detector; CC, coincidence counter; PA, polarization analyzer; $\theta_{C,L}$, polarization angles for C and L band photons.(c) Electron microscope image of a PCF used in PCF-based photon pair sources. Upper panel: the cross-section view of the photonic crystal structure. Lower panel: close-up view of the core region of the PCF. Reproduced with permission from[117] , Copyright 2005 The Optical Society of America. Reproduced with permission from[126], Copyright 2012 American Physical Society; Reproduced with permission from[114], licensed under a Creative Commons Attribution (CC-BY) license.

2. *Microresonators*

In the last decade, following the rapid development of micro-ring resonators, they have become a new option to further improve on-chip SFWM photon-pair sources. With their ultra-high Q-factor, they are naturally suited for many other applications including filtering[224], active modulation, sensing[225] and frequency comb generation[226].

Due to the high Q-factor of low-loss ring resonators and the possibility of resonant enhancement of all the three wave components (pump, signal and idler) in the FWM process. The pair generation rate r could enhanced according to the following relation[136]:

$$r = (F_p^2 F_s F_i) r_{\mathrm{ch}}, \tag{27}$$

where $F_{\mathrm{p,s,i}}$ are the field enhancement factors for pump, signal and idler frequencies and r_{ch} is the pair generation rate in a channel waveguide with length equal to the perimeter of the ring resonator. This relation implies that the pair generation rate could be strongly enhanced by the resonant FWM process in a properly designed MRR.

Early works of MRR-based photon pair generation demonstrated a significant improvement of efficiency by 2 orders of magnitude compared to simple channel waveguides, achieving a high brightness of 5 MHz/mW/nm and CAR larger than 250[136,144]. Reverse biasing of the silicon waveguide was demonstrated to mitigate the effects of free-carrier absorption, further improving the PGR to 123 MHz (corresponds to a brightness of 640 MHz/mW/nm)[145]. In a MRR with a Q-factor of 9×10^5, at a low pump power of 10 μW, CAR up to 12000 was demonstrated[157]. Exploiting multiple resonances of the MRR and broad phase-matching range, correlated photon pairs could be generated via SFWM in multiple neighboring channels[151]. The potential of photon pair sources based on silicon photonics for QPIC has been shown in its

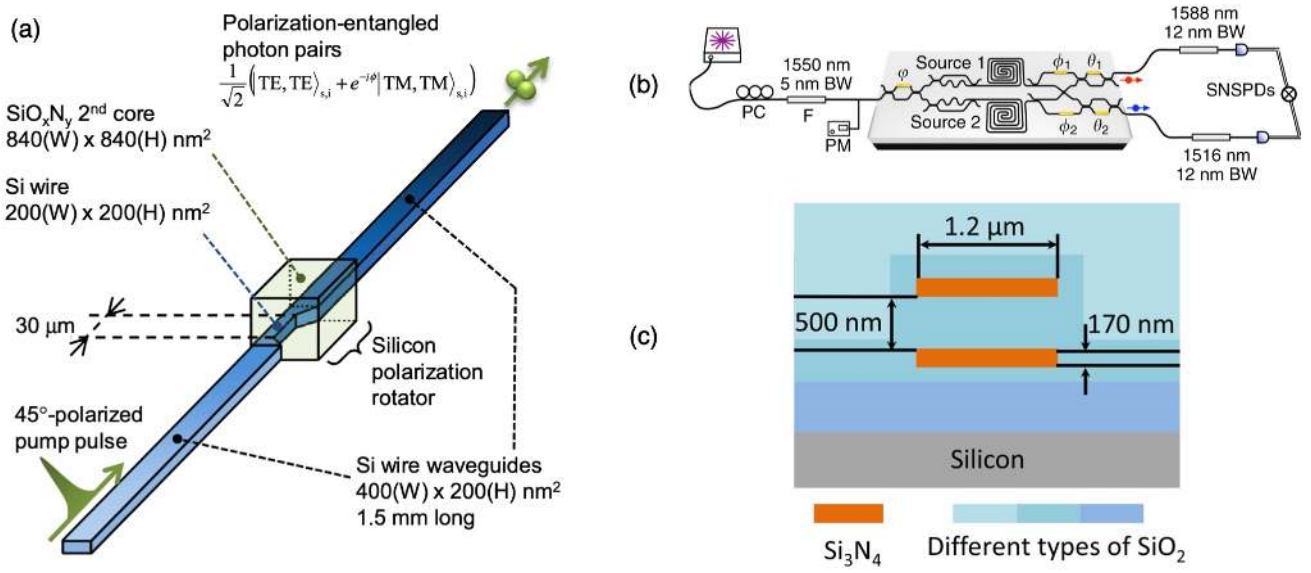

FIG. 4. Commonly used channel waveguide geometries for photon pair generation. (a) Polarization-entangled photon pair source based on silicon channel waveguide. With the addition of a symmetric Si wire section, the polarization state can be precisely controlled and produce the polarization-entangled photon pairs. TE, transverse electric; TM, transverse magnetic; W, width; H, height. (b) Path-entangled photon pair source realized with two spiral channel waveguides, on-chip directional couplers and phase shifters, showcasing the potential of system-scale integration in the near future. PPSF, periodically poled silica fiber; PC, polarization controller; F, filter; BW, bandwidth; PM, power meter; φ, $\phi_{1,2}$ and $\theta_{1,2}$, phase shifters; SNSPD, superconducting nanowire single photon detector. (c) Photon pair source based on a double-stripe waveguide geometry for the optimization of mode profile and waveguide dispersion. The advanced fabrication capabilities enables integration of different types of silicon dioxide for dispersion engineering. Reproduced with permission from[140], licensed under a Creative Commons Attribution (CC-BY) license. Reproduced with permission from[138], licensed under a Creative Commons Attribution (CC-BY) license. Reproduced with permission from[37], Copyright 2015 The Optical Society of America.

compatibility with standard CMOS fabrication processes[148] and capability for advanced functionalities such as spectral filtering systems[150,152]. Two-photon entanglement was also demonstrated in silicon MRR using energy-time/time-bin entanglement[154–157,159] and path entanglement[153,158,160] schemes with V_{TPI} up to 98%[155] (an example of entangled photon pair source with an integrated interferometer is shown in Fig.5(a)).

With SiN MRRs, time-bin/energy-time[171,173] and high-dimensional frequency-bin[172] entangled states were also generated with a brightness of 150 MHz/nm/mW[171]. Thanks to the wider bandgap and ultra-low losses of SiN, time-energy entangled photon pairs were generated also in the visible range with a CAR as high as 3780[174].

Besides the aforementioned platforms that attracted more attention, photon pair generation has been also demonstrated in other materials based MRRs. For example, MRRs were also realized in AlN demonstrating photon pair generation via SPDC with a brightness on the level of 730 MHz/mW/nm at a CAR higher than 500 with a high degree of heralded single-photon indistinguishability[68]. Entangled photon pairs were also generated in InP membrane MRRs achieving a brightness of 91 MHz/mW/nm[203]. Furthermore, correlated pair generation was also demonstrated in amorphous hydrogenated silicon channel waveguides[210] and MRR[211] showing higher PGR compared to silicon MRRs with a similar design due to the higher Kerr nonlinearity of the hydrogenated silicon. Multi-channel correlated photon pairs were demonstrated in Hydex MRRs which have a low nonlinearity ($n_2 \approx 1.15 \times 10^{-19}$ $\mathrm{m^2W^{-1}}$) and low linear loss (<0.07 dB/cm)[62]. Employing SFMW in high-Q MRRs, correlated photon pairs with a moderate brightness of 3.5 MHz/mW/nm in multiple frequency channels of the comb structure and high-dimension frequency-bin entangled states were also generated[204–207].

3. *Other waveguide structures*

For their strong second-order nonlinearities, III-V semiconductors such as GaAs and AlGaAs are also suited for photon pair generation via SPDC processes. However, in a simple channel waveguide structure the phase-matching condition cannot be easily satisfied. To this end, BRWs have been employed to enable phase-matching between transverse-electric and transverse-magnetic modes for SPDC[34,193,194], achieving CAR as high as 141 and brightness up to 102 kHz/mW/nm[196]. polarization-entangled[198,200,201] and time-energy entangled states were demonstrated in (Al)GaAs Bragg reflection waveguides via SPDC with a highest V_{TPI} of 95% and Bell state fidelity of 97%[65,192,196].

Photon pair generation can also be enhanced by slow-light structures, such as photonic crystal waveguides and coupled-

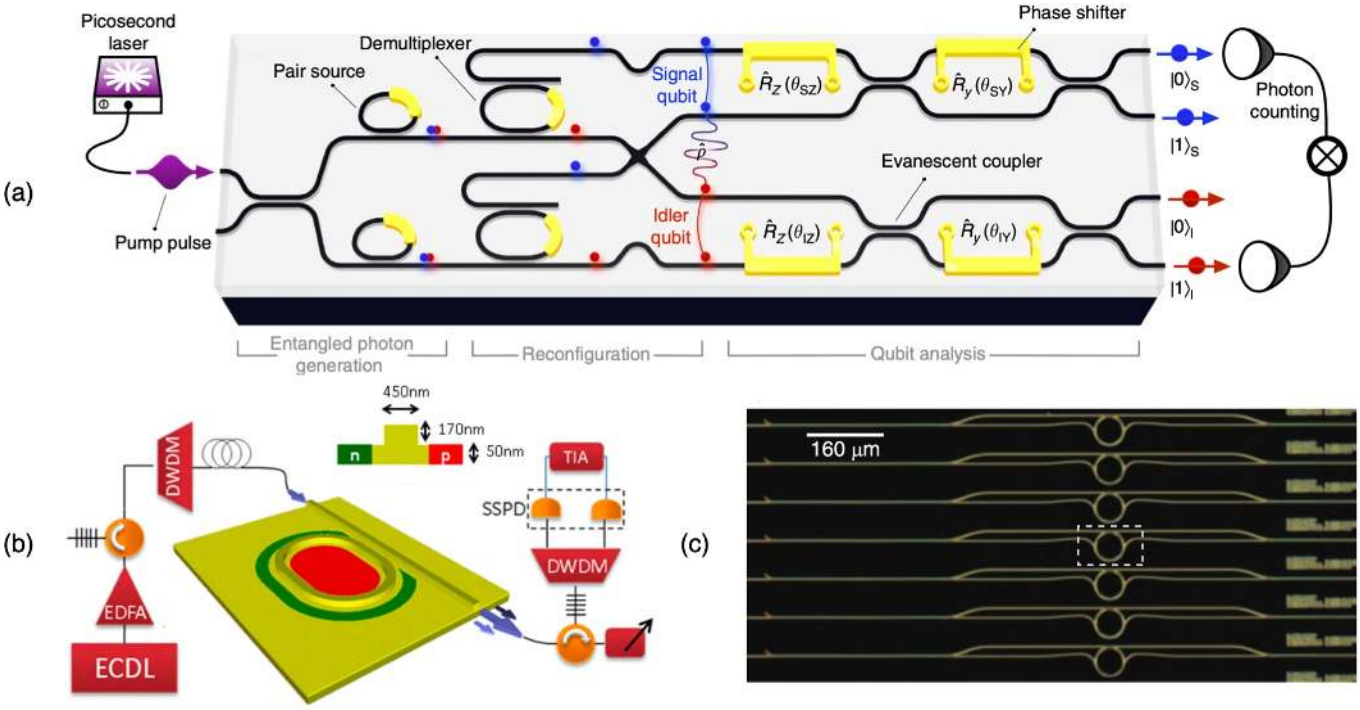

FIG. 5. Micro-ring resonators based photon pair sources. (a) A MRR based path-entangled photon pair source with integrated two-photon interferometer. Various components including directional couplers and phase shifters are integrated on-chip for the low-loss generation of entangled states. $\hat{R}_{y,z}$, phase rotations from the phase shifter for angles of $\theta_{SZ,SY,IZ,IY}$; $|0\rangle_{S,I}$, $|1\rangle_{S,I}$, states of signal and idler photons. (b) A Silicon MRR photon pair source with an integrated p-n junction (inset) for the active suppression of free-carrier effects. Further reducing losses due to TPA and free-carrier absorption are greatly beneficial for Si-based MRRs. ECDL, external cavity diode laser; DWDM, dense wavelength division multiplexer; TIA, time interval analyzer; SSPD, superconducting single photon detector. (c) An AlN MRR photon pair source based on SPDC process with on-chip WDM. The on-chip integration of tunable filters can greatly reduce the footprint of photon pair sources and the related losses. Reproduced with permission from[66], licensed under a Creative Commons Attribution (CC-BY) license. Reproduced with permission from[145], Copyright 2013 The Optical Society of America. Reproduced with permission from[153], licensed under a Creative Commons Attribution (CC-BY) license.

resonator optical waveguides. These structures are shown to possess much higher nonlinear coefficients than simple channel waveguides and MRRs[163,227]. Both correlated photon pairs[162,164–167], time-bin entangled[168] and path entangled[228] two-photon states have been demonstrated in silicon slow-light structures. Although at the moment their performances in terms of PGR (13 kHz)[229], CAR (80)[229] and V_{TPI} (74%)[168] do not compare favorably towards other types of waveguide structures, these devices have very small footprints and high efficiencies, beneficial for dense large-scale integration.

IV. PERSPECTIVES

Although research on integrated photon-pair sources with nonlinear optics has seen rapid growth and great success, further improvements in efficiency and strategies to overcome the limitations imposed by the probabilistic nature of the parametric process at a system level are in urgent need before they can be ready for realistic applications. Moreover, the development of high-performance on-chip photon pair sources can potentially lead to various exciting technological applications.

A. New material platforms

For future implementation of complex QPICs, the reduction of losses in each of the active and passive components, such as directional couplers, modulators, detectors etc., are of significant importance and have seen tremendous advances. At the same time, new materials other than those previously discussed are also under investigation. For example, with the availability of quantum memories based on nitrogen-vacancy (NV) centers, diamond has attracted considerable attention in recent years[231]. With the advance of laser inscription of waveguide[232], diamond has also been considered for integrated nonlinear optics[233] and mid-IR applications[234]. Lithium niobate with micrometer level thickness has been considered for phase-matching-free photon pair generation[235]. Other materials (such as AlN[58] and metal chalcogenides[236]) also have potentials as platforms for integrated photon pair sources.

In recent years, low-dimensional nanomaterials (for example 1D materials such as carbon nanotubes[237] and nanowires[238], 2D materials such as graphene, transition metal dichalcogenide monolayers[239–241]) have attracted considerable research efforts. Their interesting potential in nonlin-

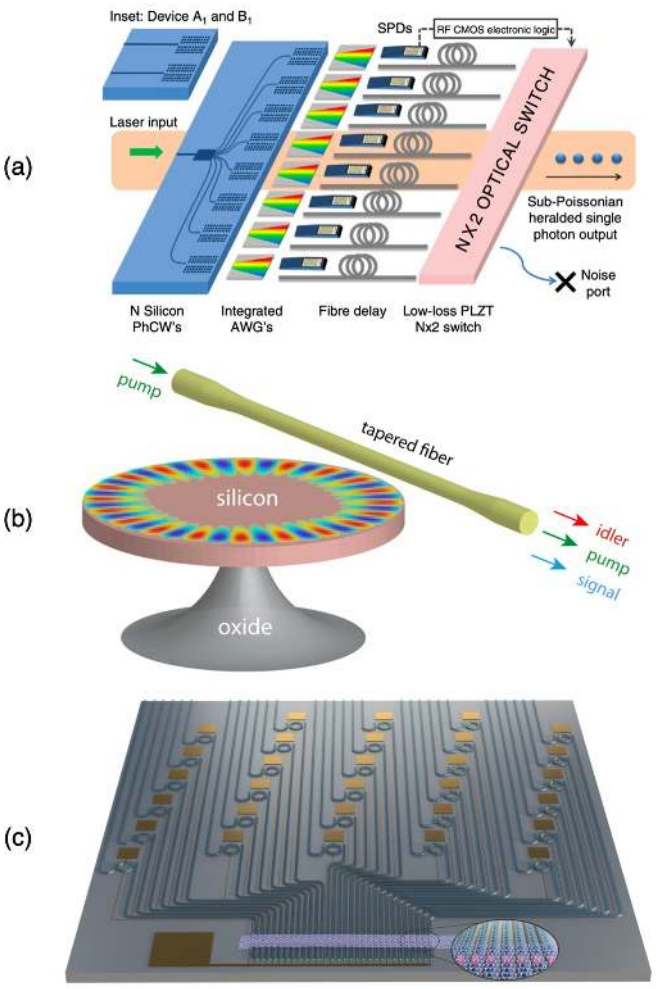

FIG. 6. Potential future developments of integrated photon pair sources from different aspects: (a) tackling the limitation due to the probabilistic nature by large-scale integration of actively multiplexed photon pair sources, (b) further improving generation efficiency by the use of high-Q resonators and low-loss tapered fiber for coupling and (c) innovation on the material platform through heterogeneous integration of 2D materials. 2D materials can be integrated with low-loss waveguides for different functionalities including as single photon emitters (inset), as nonlinear materials or as modulators and detectors. Reproduced with permission from[98], licensed under a Creative Commons Attribution (CC-BY) license. Reproduced with permission from[149], Copyright 2016 The Optical Society of America. Reproduced with permission from[230], licensed under a Creative Commons Attribution (CC-BY) license.

ear optics and quantum photonics is being gradually discovered and investigated (e.g., optical parametric generation[242] and gate tunable nonlinearity[243]). Their hybrid integration in conventional photonic waveguide platform is also under active research (as illustrated in Fig.6(c))[230]. With graphene and graphene oxide[244] deposited on top of silicon[245,246] and silicon nitride[247] waveguides and optical fibers[248,249], the effective Kerr nonlinearity of the composite waveguide structure were shown be strongly enhanced. Photon pair generation in graphene-covered silicon waveguide were also investigated. Although the nonlinearity of the waveguide was enhanced by a factor up to 10, the linear propagation loss due to absorption in graphene limits its performance in terms of PGR and CAR of the device[250]. These losses can be avoided by using transition metal dichalcogenide monolayers which are absent of the wavelength-independent absorption characteristic of semi-metallic graphene. Besides the enhancement in nonlinearity, these atomically-thin materials could also bring new functionalities such as ultrafast modulators[251] and broadband photodetectors[252].

B. Novel integrated structures

Various techniques have been investigated to further enhance the conversion efficiency of the photon-pair generation processes. Resonant cavities and structures are among the most evident solution for passive field enhancement which directly leads to increased efficiency. MRRs, photonic crystal waveguides and coupled-resonator optical waveguides have been the most widely used solution for their ultra-high Q-factor and facile integration with on-chip photonic waveguides, deserving further investigation for practical applications.

Microcavities other than MRRs such as microtoroids[253] and microdisks[146,149,254,255] could provide even higher Q-factors and potentially can further improve the efficiency of photon pair sources. Linear cavities realized with dielectric mirrors could also be employed for channel waveguides[187,256,257].

Novel metamaterials and metasurfaces[258,259] including plasmonic nanostructures[260] have also been considered for photon pair generation to take advantage of their sub-wavelength field localization. Photon pair generation via SPDC has been demonstrated in AlGaAs dielectric nanoantenna[261] and hybrid nanoantenna[262]. Metasurfaces are also being investigated for the enhancement of photon pair generation via SPDC process[263].

C. Emerging technological innovations

The utmost challenge for photon-pair sources at the moment is how they can meet the need of quantum sources with on-demand emission. The maximum probability of one single pair being emitted from a SPDC process is shown to be 25%[100]. As a result, the parametric photon pair source cannot behave as a deterministic quantum light source (as opposed to sources based on e.g. quantum dots[264]). The solution to this limitation is one of the focuses of active research endeavors in the field. Currently temporal[99,265–267], spatial[98,268] and frequency[269] multiplexing techniques are among the most common solutions, realized in free space, fibers or on-chip PICs (shown in Fig.6(a)). By multiplexing 40 channels actively in the time-domain, a single-photon probability up to 66.7%[99] was achieved recently, with the potential to maintain high purity of entanglement states[267]. With the rapid advances of large-scale photonic integration[270,271] and ultra-low

loss waveguides[53,272] near-ideal on-chip multiplexed photon-pair sources should be fathomable in the near future.

The generation of high-dimension photon states is also one of the forefronts. With the ability of generating frequency-bin high-dimensional entangled states[172,205,273,274], the quantum frequency combs[275] based on MRRs have great potentials for the generation and the control of complex photon states on a scalable integrated platform.

With the advance in integrated near-deterministic photon pair source development, the implementation of many proposals of quantum technologies on integrated photonic platforms will become closer to reality. The simulation of quantum mechanical problems could be achieved on integrated photonic platforms[276]. Quantum computation using photon qubit/qudits can be implemented with quantum walk[277], boson sampling[278–280], linear optics[281] or with cluster states in a measurement-based one-way photonic quantum computer[282,283].

V. CONCLUSION

In conclusion, we reviewed the recent advances in integrated photon-pair sources based on nonlinear parametric processes. Developments in the hybrid integration of multiple materials will bring new degrees of freedom and functionalities to the current QPIC platforms. With large-scale integration of spatial and temporal multiplexing systems, near-deterministic entangled multi-photon states can be implemented with high brightness and high-fidelity entanglement. These scalable and efficient integrated quantum light sources will be instrumental for the development and application of quantum technology in quantum key distribution for secure communication, quantum information processing, quantum metrology and sensing.

ACKNOWLEDGMENTS

The authors thank funding from Aalto Centre for Quantum Engineering, Business Finland (A-Photonics), Academy of Finland (Grant Nos. 295777, 304666, 312297, 312551, and 314810), Academy of Finland Flagship Programme (Grant No. 320167, PREIN), the European Union's Horizon 2020 research and innovation program (Grant No. 820423, S2QUIP), EU H2020-MSCA-RISE-872049 (IPN-Bio), and ERC (Grant No. 834742).

DATA AVAILABILITY

Data sharing is not applicable to this article as no new data were created or analyzed in this study.

[1] J. L. O'brien, A. Furusawa, and J. Vučković, "Photonic quantum technologies," Nature Photonics **3**, 687 (2009).
[2] J. Wang, F. Sciarrino, A. Laing, and M. G. Thompson, "Integrated photonic quantum technologies," Nature Photonics , 1–12 (2019).
[3] J. P. Dowling and G. J. Milburn, "Quantum technology: the second quantum revolution," Philosophical Transactions of the Royal Society of London. Series A: Mathematical, Physical and Engineering Sciences **361**, 1655–1674 (2003).
[4] M. A. Nielsen and I. Chuang, "Quantum computation and quantum information," (2000).
[5] V. Giovannetti, S. Lloyd, and L. Maccone, "Advances in quantum metrology," Nature photonics **5**, 222 (2011).
[6] A. Steane, "Quantum computing," Reports on Progress in Physics **61**, 117 (1998).
[7] J. L. O'brien, "Optical quantum computing," Science **318**, 1567–1570 (2007).
[8] C. L. Degen, F. Reinhard, and P. Cappellaro, "Quantum sensing," Reviews of modern physics **89**, 35002 (2017).
[9] S. Pirandola, B. R. Bardhan, T. Gehring, C. Weedbrook, and S. Lloyd, "Advances in photonic quantum sensing," Nature Photonics **12**, 724–733 (2018).
[10] N. Gisin and R. Thew, "Quantum communication," Nature photonics **1**, 165 (2007).
[11] A. W. Elshaari, W. Pernice, K. Srinivasan, O. Benson, and V. Zwiller, "Hybrid integrated quantum photonic circuits," Nature Photonics , 1–14 (2020).
[12] J.-H. Kim, S. Aghaeimeibodi, J. Carolan, D. Englund, and E. Waks, "Hybrid integration methods for on-chip quantum photonics," Optica **7**, 291–308 (2020).
[13] S. Tanzilli, A. Martin, F. Kaiser, M. P. De Micheli, O. Alibart, and D. B. Ostrowsky, "On the genesis and evolution of integrated quantum optics," Laser & Photonics Reviews **6**, 115–143 (2012).
[14] A. S. Mayer and B. C. Kirkpatrick, "Silicon photonics," Frontiers in Modern Optics **24**, 189–205 (2016).
[15] J. Leuthold, C. Koos, and W. Freude, "Nonlinear silicon photonics," Nature Photonics **4**, 535–544 (2010).
[16] J. W. Silverstone, D. Bonneau, J. L. O'Brien, and M. G. Thompson, "Silicon Quantum Photonics," IEEE Journal of Selected Topics in Quantum Electronics **22**, 390–402 (2016).
[17] S. Bogdanov, M. Y. Shalaginov, A. Boltasseva, and V. M. Shalaev, "Material platforms for integrated quantum photonics," Optical Materials Express **7**, 111–132 (2017).
[18] M. D. Eisaman, J. Fan, A. Migdall, and S. V. Polyakov, "Invited review article: Single-photon sources and detectors," Review of scientific instruments **82**, 71101 (2011).
[19] L. Caspani, C. Xiong, B. J. Eggleton, D. Bajoni, M. Liscidini, M. Galli, R. Morandotti, and D. J. Moss, "Integrated sources of photon quantum states based on nonlinear optics," Light: Science & Applications **6**, e17100—-e17100 (2017).
[20] A. Orieux, M. A. M. Versteegh, K. D. Jöns, and S. Ducci, "Semiconductor devices for entangled photon pair generation: a review," Reports on Progress in Physics **80**, 76001 (2017).
[21] R. W. Boyd, Nonlinear optics (Academic press, 2010).
[22] L. Caspani, C. Xiong, B. J. Eggleton, D. Bajoni, M. Liscidini, M. Galli, R. Morandotti, and D. J. Moss, "Integrated sources of photon quantum states based on nonlinear optics," Light: Science and Applications **6**, e17100–12 (2017).
[23] Q. Lin, O. J. Painter, and G. P. Agrawal, "Nonlinear optical phenomena in silicon waveguides: Modeling and applications," Opt. Express **15**, 16604–16644 (2007).
[24] C. Couteau, "Spontaneous parametric down-conversion," Contemporary Physics **59**, 291–304 (2018), arXiv:1809.00127.
[25] X. Cheng, M. C. Sarihan, K.-C. Chang, Y. S. Lee, F. Laudenbach, H. Ye, Z. Yu, and C. W. Wong, "Design of spontaneous parametric down-conversion in integrated hybrid sixny-ppln waveguides," Opt. Express **27**, 30773–30787 (2019).
[26] A. Ling, A. Lamas-Linares, and C. Kurtsiefer, "Absolute emission rates of spontaneous parametric down-conversion into single transverse gaussian modes," Phys. Rev. A **77**, 043834 (2008).
[27] Q. Lin, F. Yaman, and G. P. Agrawal, "Photon-pair generation in optical fibers through four-wave mixing: Role of Raman scattering and pump polarization," Physical Review A **75**, 23803 (2007).
[28] L. J. Wang, C. K. Hong, and S. R. Friberg, "Generation of correlated photons via four-wave mixing in optical fibres," Journal of Optics B: Quantum

and Semiclassical Optics **3**, 346–352 (2001).
[29]Q. Lin, F. Yaman, and G. P. Agrawal, "Photon-pair generation in optical fibers through four-wave mixing: Role of Raman scattering and pump polarization," Physical Review A - Atomic, Molecular, and Optical Physics **75**, 1–20 (2007).
[30]R. S. Jacobsen, K. N. Andersen, P. I. Borel, J. Fage-Pedersen, L. H. Frandsen, O. Hansen, M. Kristensen, A. V. Lavrinenko, G. Moulin, H. Ou, C. Peucheret, B. Zsigri, and A. Bjarklev, "Strained silicon as a new electro-optic material," Nature **441**, 199–202 (2006).
[31]X. Lu, G. Moille, A. Rao, D. Westly, and K. Srinivasan, "Efficient photoinduced second harmonic generation in silicon photonics," arXiv preprint arXiv:2003.12176 (2020).
[32]L. Du, Y. Dai, and Z. Sun, "Twisting for tunable nonlinear optics," Matter **3**, 987 – 988 (2020).
[33]S. Tanzilli, H. De Riedmatten, W. Tittel, H. Zbinden, P. Baldi, M. De Micheli, D. B. Ostrowsky, and N. Gisin, "Highly efficient photon-pair source using periodically poled lithium niobate waveguide," Electronics Letters **37**, 26–28 (2001).
[34]X. Caillet, A. Orieux, A. Lemaître, P. Filloux, I. Favero, G. Leo, and S. Ducci, "Two-photon interference with a semiconductor integrated source at room temperature," Optics express **18**, 9967–9975 (2010).
[35]J. W. Silverstone, J. Wang, D. Bonneau, P. Sibson, R. Santagati, C. Erven, J. L. O'Brien, and M. G. Thompson, "Silicon quantum photonics," in 2016 International Conference on Optical MEMS and Nanophotonics (OMN) (IEEE, 2016) pp. 1–2.
[36]H. Takesue, Y. Tokura, H. Fukuda, T. Tsuchizawa, T. Watanabe, K. Yamada, and S.-i. Itabashi, "Entanglement generation using silicon wire waveguide," Applied Physics Letters **91**, 201108 (2007).
[37]C. Xiong, X. Zhang, A. Mahendra, J. He, D.-Y. Choi, C. J. Chae, D. Marpaung, A. Leinse, R. G. Heideman, M. Hoekman, C. G. H. Roeloffzen, R. M. Oldenbeuving, P. W. L. van Dijk, C. Taddei, P. H. W. Leong, and B. J. Eggleton, "Compact and reconfigurable silicon nitride time-bin entanglement circuit," Optica **2**, 724–727 (2015).
[38]S. Atzeni, A. S. Rab, G. Corrielli, E. Polino, M. Valeri, P. Mataloni, N. Spagnolo, A. Crespi, F. Sciarrino, and R. Osellame, "Integrated sources of entangled photons at the telecom wavelength in femtosecond-laser-written circuits," Optica **5**, 311–314 (2018).
[39]R. A. Soref and J. P. Lorenzo, "Single-crystal silicon: a new material for 1.3 and 1.6 μm integrated-optical components," Electronics Letters **21**, 953–954 (1985).
[40]R. Soref, "The past, present, and future of silicon photonics," IEEE Journal of selected topics in quantum electronics **12**, 1678–1687 (2006).
[41]D. Thomson, A. Zilkie, J. E. Bowers, T. Komljenovic, G. T. Reed, L. Vivien, D. Marris-Morini, E. Cassan, L. Virot, J.-M. Fédéli, J.-M. Hartmann, J. H. Schmid, D.-X. Xu, F. Boeuf, P. O'Brien, G. Z. Mashanovich, and M. Nedeljkovic, "Roadmap on silicon photonics," Journal of Optics **18**, 73003 (2016).
[42]J. Leuthold, C. Koos, and W. Freude, "Nonlinear silicon photonics," Nature photonics **4**, 535–544 (2010).
[43]M. Cazzanelli, F. Bianco, E. Borga, G. Pucker, M. Ghulinyan, E. Degoli, E. Luppi, V. Véniard, S. Ossicini, D. Modotto, S. Wabnitz, R. Pierobon, and L. Pavesi, "Second-harmonic generation in silicon waveguides strained by silicon nitride," Nature materials **11**, 148–154 (2012).
[44]H. K. Tsang and Y. Liu, "Nonlinear optical properties of silicon waveguides," Semiconductor Science and Technology **23**, 64007 (2008).
[45]T. Vallaitis, S. Bogatscher, L. Alloatti, P. Dumon, R. Baets, M. L. Scimeca, I. Biaggio, F. Diederich, C. Koos, W. Freude, and J. Leuthold, "Optical properties of highly nonlinear silicon-organic hybrid (SOH) waveguide geometries," Optics express **17**, 17357–17368 (2009).
[46]A. Rahim, E. Ryckeboer, A. Z. Subramanian, S. Clemmen, B. Kuyken, A. Dhakal, A. Raza, A. Hermans, M. Muneeb, S. Dhoore, Y. Li, U. Dave, P. Bienstman, N. L. Thomas, G. Roelkens, D. V. Thourhout, P. Helin, S. Severi, X. Rottenberg, and R. Baets, "Expanding the silicon photonics portfolio with silicon nitride photonic integrated circuits," Journal of lightwave technology **35**, 639–649 (2017).
[47]M. H. P. Pfeiffer, J. Liu, A. S. Raja, T. Morais, B. Ghadiani, and T. J. Kippenberg, "Ultra-smooth silicon nitride waveguides based on the Damascene reflow process: fabrication and loss origins," Optica **5**, 884–892 (2018).
[48]K. Luke, A. Dutt, C. B. Poitras, and M. Lipson, "Overcoming Si 3 N 4 film stress limitations for high quality factor ring resonators," Optics express **21**, 22829–22833 (2013).
[49]K. Alexander, J. P. George, J. Verbist, K. Neyts, B. Kuyken, D. Van Thourhout, and J. Beeckman, "Nanophotonic Pockels modulators on a silicon nitride platform," Nature communications **9**, 3444 (2018).
[50]G.-R. Lin, S.-P. Su, C.-L. Wu, Y.-H. Lin, B.-J. Huang, H.-Y. Wang, C.-T. Tsai, C.-I. Wu, and Y.-C. Chi, "Si-rich SiN x based Kerr switch enables optical data conversion up to 12 Gbit/s," Scientific reports **5**, 9611 (2015).
[51]D. Ahn, C.-y. Hong, J. Liu, W. Giziewicz, M. Beals, L. C. Kimerling, J. Michel, J. Chen, and F. X. Kärtner, "High performance, waveguide integrated Ge photodetectors," Optics express **15**, 3916–3921 (2007).
[52]M. Dinu, F. Quochi, and H. Garcia, "Third-order nonlinearities in silicon at telecom wavelengths," Applied physics letters **82**, 2954–2956 (2003).
[53]G. Li, J. Yao, H. Thacker, A. Mekis, X. Zheng, I. Shubin, Y. Luo, J. hyoung Lee, K. Raj, J. E. Cunningham, and A. V. Krishnamoorthy, "Ultralow-loss, high-density SOI optical waveguide routing for macrochip interconnects," Optics express **20**, 12035–12039 (2012).
[54]I. Shoji, T. Kondo, and R. Ito, "Second-order nonlinear susceptibilities of various dielectric and semiconductor materials," Optical and Quantum Electronics **34**, 797–833 (2002).
[55]Y. Sugimoto, Y. Tanaka, N. Ikeda, Y. Nakamura, K. Asakawa, and K. Inoue, "Low propagation loss of 0.76 dB/mm in GaAs-based single-line-defect two-dimensional photonic crystal slab waveguides up to 1 cm in length," Optics Express **12**, 1090–1096 (2004).
[56]Y. Fujii, S. Yoshida, S. Misawa, S. Maekawa, and T. Sakudo, "Nonlinear optical susceptibilities of aln film," Applied Physics Letters **31**, 815–816 (1977).
[57]H. Jung, C. Xiong, K. Y. Fong, X. Zhang, and H. X. Tang, "Optical frequency comb generation from aluminum nitride microring resonator," Optics letters **38**, 2810–2813 (2013).
[58]C. Xiong, W. H. P. Pernice, X. Sun, C. Schuck, K. Y. Fong, and H. X. Tang, "Aluminum nitride as a new material for chip-scale optomechanics and nonlinear optics," New Journal of Physics **14**, 95014 (2012).
[59]R. DeSalvo, A. A. Said, D. J. Hagan, E. W. Van Stryland, and M. Sheik-Bahae, "Infrared to ultraviolet measurements of two-photon absorption and n/sub 2/in wide bandgap solids," IEEE Journal of Quantum Electronics **32**, 1324–1333 (1996).
[60]H. T. Bookey, R. R. Thomson, N. D. Psaila, A. K. Kar, N. Chiodo, R. Osellame, and G. Cerullo, "Femtosecond Laser Inscription of Low Insertion Loss Waveguides in Z-Cut Lithium Niobate," IEEE Photonics Technology Letters **19**, 892–894 (2007).
[61]D. Milam, "Review and assessment of measured values of the nonlinear refractive-index coefficient of fused silica," Applied optics **37**, 546–550 (1998).
[62]D. J. Moss, R. Morandotti, A. L. Gaeta, and M. Lipson, "New CMOS-compatible platforms based on silicon nitride and Hydex for nonlinear optics," Nature photonics **7**, 597–607 (2013).
[63]C. P. Dietrich, A. Fiore, M. G. Thompson, M. Kamp, and S. Höfling, "GaAs integrated quantum photonics: Towards compact and multi-functional quantum photonic integrated circuits," Laser & Photonics Reviews **10**, 870–894 (2016).
[64]R. G. Walker, "High-speed III-V semiconductor intensity modulators," IEEE Journal of Quantum Electronics **27**, 654–667 (1991).
[65]A. Orieux, A. Eckstein, A. Lemaître, P. Filloux, I. Favero, G. Leo, T. Coudreau, A. Keller, P. Milman, and S. Ducci, "Direct Bell states generation on a III-V semiconductor chip at room temperature," Physical review letters **110**, 160502 (2013).
[66]P. Kultavewuti, E. Y. Zhu, X. Xing, L. Qian, V. Pusino, M. Sorel, and J. S. Aitchison, "Polarization-entangled photon pair sources based on spontaneous four wave mixing assisted by polarization mode dispersion," Scientific reports **7**, 1–10 (2017).
[67]F. Boitier, A. Orieux, C. Autebert, A. Lemaître, E. Galopin, C. Manquest, C. Sirtori, I. Favero, G. Leo, and S. Ducci, "Electrically injected photon-pair source at room temperature," Physical review letters **112**, 183901 (2014).
[68]X. Guo, C.-l. Zou, C. Schuck, H. Jung, R. Cheng, and H. X. Tang, "Parametric down-conversion photon-pair source on a nanophotonic chip," Light: Science & Applications **6**, e16249—-e16249 (2017).

[69]K. D. Jöns, L. Schweickert, M. A. Versteegh, D. Dalacu, P. J. Poole, A. Gulinatti, A. Giudice, V. Zwiller, and M. E. Reimer, "Bright nanoscale source of deterministic entangled photon pairs violating bell's inequality," Scientific Reports **7**, 1–11 (2017).
[70]L. Arizmendi, "Photonic applications of lithium niobate crystals," physica status solidi (a) **201**, 253–283 (2004).
[71]R. R. Gattass and E. Mazur, "Femtosecond laser micromachining in transparent materials," Nature photonics **2**, 219–225 (2008).
[72]M. Armenise, "Fabrication techniques of lithium niobate waveguides," IEE Proceedings J (Optoelectronics) **135**, 85–91 (1988).
[73]O. Alibart, V. D'Auria, M. D. Micheli, F. Doutre, F. Kaiser, L. Labonté, T. Lunghi, É. Picholle, and S. Tanzilli, "Quantum photonics at telecom wavelengths based on lithium niobate waveguides," Journal of Optics (United Kingdom) **18** (2016), 10.1088/2040-8978/18/10/104001, arXiv:1608.01100.
[74]C. Schuck, W. H. Pernice, and H. X. Tang, "Waveguide integrated low noise nbtin nanowire single-photon detectors with milli-hz dark count rate," Scientific reports **3**, 1893 (2013).
[75]A. A. Sayem, R. Cheng, S. Wang, and H. X. Tang, "Lithium-niobate-on-insulator waveguide-integrated superconducting nanowire single-photon detectors," Applied Physics Letters **116**, 151102 (2020).
[76]G. Poberaj, H. Hu, W. Sohler, and P. Günter, "Lithium niobate on insulator (LNOI) for micro-photonic devices," Laser and Photonics Reviews **6**, 488–503 (2012).
[77]M. Bazzan and C. Sada, "Optical waveguides in lithium niobate: Recent developments and applications," Applied Physics Reviews **2**, 40603 (2015).
[78]C. Xiong, G. D. Marshall, A. Peruzzo, M. Lobino, A. S. Clark, D.-Y. Choi, S. J. Madden, C. M. Natarajan, M. G. Tanner, R. H. Hadfield, S. N. Dorenbos, T. Zijlstra, V. Zwiller, M. G. Thompson, J. G. Rarity, M. J. Steel, B. Luther-Davies, B. J. Eggleton, and J. L. O'Brien, "Generation of correlated photon pairs in a chalcogenide As 2 S 3 waveguide," Applied Physics Letters **98**, 51101 (2011).
[79]J. S. Sanghera, L. B. Shaw, and I. D. Aggarwal, "Chalcogenide glass-fiber-based mid-ir sources and applications," IEEE Journal of Selected Topics in Quantum Electronics **15**, 114–119 (2009).
[80]C. R. Petersen, U. Møller, I. Kubat, B. Zhou, S. Dupont, J. Ramsay, T. Benson, S. Sujecki, N. Abdel-Moneim, Z. Tang, D. Furniss, A. Seddon, and O. Bang, "Mid-infrared supercontinuum covering the 1.4–13.3 μm molecular fingerprint region using ultra-high na chalcogenide step-index fibre," Nature Photonics **8**, 830–834 (2014).
[81]S. O. Leonov, Y. Wang, V. S. Shiryaev, G. E. Snopatin, B. S. Stepanov, V. G. Plotnichenko, E. Vicentini, A. Gambetta, N. Coluccelli, C. Svelto, P. Laporta, and G. Galzerano, "Coherent mid-infrared supercontinuum generation in tapered suspended-core as 39 se 61 fibers pumped by a few-optical-cycle cr: Znse laser," Optics Letters **45**, 1346–1349 (2020).
[82]M. Fox, Quantum optics: an introduction, Vol. 15 (OUP Oxford, 2006).
[83]L.-T. Feng, G.-C. Guo, and X.-F. Ren, "Progress on integrated quantum photonic sources with silicon," Advanced Quantum Technologies **3**, 1900058 (2020).
[84]K. Harada, H. Takesue, H. Fukuda, T. Tsuchizawa, T. Watanabe, K. Yamada, Y. Tokura, and S. Itabashi, "Frequency and polarization characteristics of correlated photon-pair generation using a silicon wire waveguide," IEEE Journal of Selected Topics in Quantum Electronics **16**, 325–331 (2010).
[85]O. Alibart, J. Fulconis, G. K. L. Wong, S. G. Murdoch, W. J. Wadsworth, and J. G. Rarity, "Photon pair generation using four-wave mixing in a microstructured fibre: theory versus experiment," New Journal of Physics **8**, 67 (2006).
[86]C. K. Hong, Z. Y. Ou, and L. Mandel, "Measurement of subpicosecond time intervals between two photons by interference," Phys. Rev. Lett. **59**, 2044–2046 (1987).
[87]J. D. Franson, "Bell inequality for position and time," Physical review letters **62**, 2205 (1989).
[88]J. F. Clauser, M. A. Horne, A. Shimony, and R. A. Holt, "Proposed experiment to test local hidden-variable theories," Physical review letters **23**, 880 (1969).
[89]S. Aerts, P. Kwiat, J.-A. Larsson, and M. Z˙ukowski, "Two-photon franson-type experiments and local realism," Phys. Rev. Lett. **83**, 2872–2875 (1999).
[90]K. Zielnicki, K. Garay-Palmett, D. Cruz-Delgado, H. Cruz-Ramirez, M. F. O'Boyle, B. Fang, V. O. Lorenz, A. B. U'Ren, and P. G. Kwiat, "Joint spectral characterization of photon-pair sources," Journal of Modern Optics **65**, 1141–1160 (2018).
[91]B. Brecht, D. V. Reddy, C. Silberhorn, and M. G. Raymer, "Photon temporal modes: A complete framework for quantum information science," Phys. Rev. X **5**, 041017 (2015).
[92]J. B. Spring, P. S. Salter, B. J. Metcalf, P. C. Humphreys, M. Moore, N. Thomas-Peter, M. Barbieri, X.-M. Jin, N. K. Langford, W. S. Kolthammer, M. J. Booth, and I. A. Walmsley, "On-chip low loss heralded source of pure single photons," Opt. Express **21**, 13522–13532 (2013).
[93]G. Harder, V. Ansari, B. Brecht, T. Dirmeier, C. Marquardt, and C. Silberhorn, "An optimized photon pair source for quantum circuits," Opt. Express **21**, 13975–13985 (2013).
[94]X.-s. Ma, S. Zotter, J. Kofler, T. Jennewein, and A. Zeilinger, "Experimental generation of single photons via active multiplexing," Physical Review A **83**, 43814 (2011).
[95]A. L. Migdall, D. Branning, and S. Castelletto, "Tailoring single-photon and multiphoton probabilities of a single-photon on-demand source," Phys. Rev. A **66**, 53805 (2002).
[96]M. Avenhaus, H. B. Coldenstrodt-Ronge, K. Laiho, W. Mauerer, I. A. Walmsley, and C. Silberhorn, "Photon number statistics of multimode parametric down-conversion," Phys. Rev. Lett. **101**, 053601 (2008).
[97]I. Aharonovich, D. Englund, and M. Toth, "Solid-state single-photon emitters," Nature Photonics **10**, 631 (2016).
[98]M. J. Collins, C. Xiong, I. H. Rey, T. D. Vo, J. He, S. Shahnia, C. Reardon, T. F. Krauss, M. J. Steel, A. S. Clark, and B. J. Eggleton, "Integrated spatial multiplexing of heralded single-photon sources," Nature communications **4**, 1–7 (2013).
[99]F. Kaneda and P. G. Kwiat, "High-efficiency single-photon generation via large-scale active time multiplexing," Science advances **5**, eaaw8586 (2019).
[100]A. Christ and C. Silberhorn, "Limits on the deterministic creation of pure single-photon states using parametric down-conversion," Phys. Rev. A **85**, 023829 (2012).
[101]D. C. Burnham and D. L. Weinberg, "Observation of simultaneity in parametric production of optical photon pairs," Physical Review Letters **25**, 84–87 (1970).
[102]B. Y. Zel'Dovich and D. N. Klyshko, "Field statistics in parametric luminescence," ZhETF Pisma Redaktsiiu **9**, 69 (1969).
[103]M. Fiorentino, P. L. Voss, J. E. Sharping, and P. Kumar, "All-fiber photon-pair source for quantum communications," IEEE Photonics Technology Letters **14**, 983–985 (2002).
[104]K. Inoue and K. Shimizu, "Generation of quantum-correlated photon pairs in optical fiber: influence of spontaneous Raman scattering," Japanese journal of applied physics **43**, 8048 (2004).
[105]L. J. Wang, C. K. Hong, and S. R. Friberg, "Generation of correlated photons via four-wave mixing in optical fibres," Journal of optics B: Quantum and semiclassical optics **3**, 346 (2001).
[106]X. Li, J. Chen, P. Voss, J. Sharping, and P. Kumar, "All-fiber photon-pair source for quantum communications: Improved generation of correlated photons," Optics express **12**, 3737–3744 (2004).
[107]H. Takesue and K. Inoue, "1.5-μm band quantum-correlated photon pair generation in dispersion-shifted fiber: suppression of noise photons by cooling fiber," Optics express **13**, 7832–7839 (2005).
[108]S. D. Dyer, B. Baek, and S. W. Nam, "High-brightness, low-noise, all-fiber photon pair source," Optics express **17**, 10290–10297 (2009).
[109]J. E. Sharping, M. Fiorentino, and P. Kumar, "Observation of twin-beam-type quantum correlation in optical fiber," Optics Letters **26**, 367 (2001).
[110]H. Takesue and K. Inoue, "Generation of polarization-entangled photon pairs and violation of Bell's inequality using spontaneous four-wave mixing in a fiber loop," Physical Review A **70**, 31802 (2004).
[111]M. Fiorentino, P. L. Voss, J. E. Sharping, and P. Kumar, "All-fiber photon-pair source for quantum communications," IEEE Photonics Technology Letters **14**, 983–985 (2002).
[112]H. Takesue and K. Inoue, "Generation of 1.5- μ m band time-bin entanglement using spontaneous fiber four-wave mixing and planar light-wave circuit interferometers," Physical Review A **72**, 041804 (2005).
[113]X. Li, P. L. Voss, J. E. Sharping, and P. Kumar, "Optical-fiber source of polarization-entangled photons in the 1550 nm telecom band," Physical

Review Letters **94**, 3086–3094 (2005), arXiv:0402191 [quant-ph].
[114] A. Clark, B. Bell, J. Fulconis, M. M. Halder, B. Cemlyn, O. Alibart, C. Xiong, W. J. Wadsworth, and J. G. Rarity, "Intrinsically narrowband pair photon generation in microstructured fibres," New Journal of Physics **13**, 65009 (2011).
[115] J. E. Sharping, J. Chen, X. Li, P. Kumar, and R. S. Windeler, "Quantum-correlated twin photons from microstructure fiber," Optics Express **12**, 3086 (2004).
[116] J. G. Rarity, J. Fulconis, J. Duligall, W. J. Wadsworth, and P. S. J. Russell, "Photonic crystal fiber source of correlated photon pairs," Optics express **13**, 534–544 (2005).
[117] J. Fulconis, O. Alibart, W. J. Wadsworth, P. S. Russell, and J. G. Rarity, "High brightness single mode source of correlated photon pairs using a photonic crystal fiber," Opt. Express **13**, 7572–7582 (2005).
[118] J. Fan, A. Migdall, and L. J. Wang, "Efficient generation of correlated photon pairs in a microstructure fiber," Optics letters **30**, 3368–3370 (2005).
[119] J. Fulconis, O. Alibart, W. J. Wadsworth, and J. G. Rarity, "Quantum interference with photon pairs using two micro-structured fibres," New Journal of Physics **9**, 276 (2007).
[120] M. Halder, J. Fulconis, B. Cemlyn, A. Clark, C. Xiong, W. J. Wadsworth, and J. G. Rarity, "Nonclassical 2-photon interference with separate intrinsically narrowband fibre sources," Optics Express **17**, 4670 (2009).
[121] J. Fan, M. D. Eisaman, and A. Migdall, "Bright phase-stable broadband fiber-based source of polarization-entangled photon pairs," Physical Review A - Atomic, Molecular, and Optical Physics **76**, 1–4 (2007).
[122] J. Fulconis, O. Alibart, J. L. O'Brien, W. J. Wadsworth, and J. G. Rarity, "Nonclassical interference and entanglement generation using a photonic crystal fiber pair photon source," Physical review letters **99**, 120501 (2007).
[123] G. Bonfrate, V. Pruneri, P. G. Kazansky, P. Tapster, and J. G. Rarity, "Parametric fluorescence in periodically poled silica fibers," Applied physics letters **75**, 2356–2358 (1999).
[124] K. P. Huy, A. T. Nguyen, E. Brainis, M. Haelterman, P. Emplit, C. Corbari, A. Canagasabey, M. Ibsen, P. G. Kazansky, O. Deparis, A. A. Fotiadi, P. Mégret, and S. Massar, "Photon pair source based on parametric fluorescence in periodically poled twin-hole silica fiber," Optics express **15**, 4419–4426 (2007).
[125] E. Y. Zhu, Z. Tang, L. Qian, L. G. Helt, M. Liscidini, J. E. Sipe, C. Corbari, A. Canagasabey, M. Ibsen, and P. G. Kazansky, "Poled-fiber source of broadband polarization-entangled photon pairs," Optics letters **38**, 4397–4400 (2013).
[126] E. Y. Zhu, Z. Tang, L. Qian, L. G. Helt, M. Liscidini, J. E. Sipe, C. Corbari, A. Canagasabey, M. Ibsen, and P. G. Kazansky, "Direct generation of polarization-entangled photon pairs in a poled fiber," Physical review letters **108**, 213902 (2012).
[127] H. Takesue, Y. Tokura, H. Fukuda, T. Tsuchizawa, T. Watanabe, K. Yamada, and S. I. Itabashi, "Entanglement generation using silicon wire waveguide," Applied Physics Letters **91**, 10–13 (2007).
[128] K.-i. Harada, H. Takesue, H. Fukuda, T. Tsuchizawa, T. Watanabe, K. Yamada, Y. Tokura, and S.-i. Itabashi, "Frequency and polarization characteristics of correlated photon-pair generation using a silicon wire waveguide," IEEE Journal of Selected Topics in Quantum Electronics **16**, 325–331 (2009).
[129] K. Guo, E. N. Christensen, J. B. Christensen, J. G. Koefoed, D. Bacco, Y. Ding, H. Ou, and K. Rottwitt, "High coincidence-to-accidental ratio continuous-wave photon-pair generation in a grating-coupled silicon strip waveguide," Applied Physics Express **10**, 62801 (2017).
[130] C. Jie-Rong, Z. Wei, Z. Qiang, F. Xue, H. Yi-Dong, and P. Jiang-De, "Correlated photon pair generation in silicon wire waveguides at 1.5 μm," Chinese Physics Letters **27**, 124208 (2010).
[131] K.-i. Harada, H. Takesue, H. Fukuda, T. Tsuchizawa, T. Watanabe, K. Yamada, Y. Tokura, and S.-i. Itabashi, "Indistinguishable photon pair generation using two independent silicon wire waveguides," New Journal of Physics **13**, 65005 (2011).
[132] J. W. Silverstone, D. Bonneau, K. Ohira, N. Suzuki, H. Yoshida, N. Iizuka, M. Ezaki, C. M. Natarajan, M. G. Tanner, R. H. Hadfield, V. Zwiller, G. D. Marshall, J. G. Rarity, J. L. O'Brien, and M. G. Thompson, "On-chip quantum interference between silicon photon-pair sources," Nature Photonics **8**, 104 (2014).
[133] J. E. Sharping, K. F. Lee, M. A. Foster, A. C. Turner, B. S. Schmidt, M. Lipson, A. L. Gaeta, and P. Kumar, "Generation of correlated photons in nanoscale silicon waveguides," Opt. Express **14**, 12388–12393 (2006).
[134] H. Takesue, H. Fukuda, T. Tsuchizawa, T. Watanabe, K. Yamada, Y. Tokura, and S.-i. Itabashi, "Generation of polarization entangled photon pairs using silicon wire waveguide," Optics express **16**, 5721–5727 (2008).
[135] K.-i. Harada, H. Takesue, H. Fukuda, T. Tsuchizawa, T. Watanabe, K. Yamada, Y. Tokura, and S.-i. Itabashi, "Generation of high-purity entangled photon pairs using silicon wire waveguide," Optics express **16**, 20368–20373 (2008).
[136] S. Clemmen, K. P. Huy, W. Bogaerts, R. G. Baets, P. Emplit, and S. Massar, "Continuous wave photon pair generation in silicon-on-insulator waveguides and ring resonators," Optics express **17**, 16558–16570 (2009).
[137] M. Zhang, L.-T. Feng, Z.-Y. Zhou, Y. Chen, H. Wu, M. Li, S.-M. Gao, G.-P. Guo, G.-C. Guo, D.-X. Dai, and X.-F. Ren, "Generation of multiphoton quantum states on silicon," Light: Science & Applications **8**, 1–7 (2019).
[138] S. Paesani, M. Borghi, S. Signorini, A. Ma\"\inos, L. Pavesi, and A. Laing, "Near-ideal spontaneous photon sources in silicon quantum photonics," Nature communications **11**, 1–6 (2020).
[139] L.-T. Feng, M. Zhang, X. Xiong, Y. Chen, H. Wu, M. Li, G.-P. Guo, G.-C. Guo, D.-X. Dai, and X.-F. Ren, "On-chip transverse-mode entangled photon pair source," npj Quantum Information **5**, 1–7 (2019).
[140] N. Matsuda, H. Le Jeannic, H. Fukuda, T. Tsuchizawa, W. J. Munro, K. Shimizu, K. Yamada, Y. Tokura, and H. Takesue, "A monolithically integrated polarization entangled photon pair source on a silicon chip," Scientific reports **2**, 817 (2012).
[141] L. Olislager, J. Safioui, S. Clemmen, K. P. Huy, W. Bogaerts, R. Baets, P. Emplit, and S. Massar, "Silicon-on-insulator integrated source of polarization-entangled photons," Optics letters **38**, 1960–1962 (2013).
[142] N. Lv, W. Zhang, Y. Guo, Q. Zhou, Y. Huang, and J. Peng, "1.5 μm polarization entanglement generation based on birefringence in silicon wire waveguides," Optics Letters **38**, 2873–2876 (2013).
[143] M. Savanier, R. Kumar, and S. Mookherjea, "Optimizing photon-pair generation electronically using a pin diode incorporated in a silicon microring resonator," Applied Physics Letters **107**, 131101 (2015).
[144] S. Azzini, D. Grassani, M. J. Strain, M. Sorel, L. G. Helt, J. E. Sipe, M. Liscidini, M. Galli, and D. Bajoni, "Ultra-low power generation of twin photons in a compact silicon ring resonator," Optics express **20**, 23100–23107 (2012).
[145] E. Engin, D. Bonneau, C. M. Natarajan, A. S. Clark, M. G. Tanner, R. H. Hadfield, S. N. Dorenbos, V. Zwiller, K. Ohira, N. Suzuki, H. Yoshida, N. Iizuka, M. Ezaki, J. L. O'Brien, and M. G. Thompson, "Photon pair generation in a silicon micro-ring resonator with reverse bias enhancement," Optics express **21**, 27826–27834 (2013).
[146] W. C. Jiang, X. Lu, J. Zhang, O. Painter, and Q. Lin, "Silicon-chip source of bright photon pairs," Optics express **23**, 20884–20904 (2015).
[147] M. Savanier, R. Kumar, and S. Mookherjea, "Photon pair generation from compact silicon microring resonators using microwatt-level pump powers," Optics express **24**, 3313–3328 (2016).
[148] C. M. Gentry, J. M. Shainline, M. T. Wade, M. J. Stevens, S. D. Dyer, X. Zeng, F. Pavanello, T. Gerrits, S. W. Nam, R. P. Mirin, and M. A. Popović, "Quantum-correlated photon pairs generated in a commercial 45 nm complementary metal-oxide semiconductor microelectronic chip," Optica **2**, 1065–1071 (2015).
[149] X. Lu, S. Rogers, T. Gerrits, W. C. Jiang, S. W. Nam, and Q. Lin, "Heralding single photons from a high-Q silicon microdisk," Optica **3**, 1331–1338 (2016).
[150] C. Ma, X. Wang, and S. Mookherjea, "Progress towards a widely usable integrated silicon photonic photon-pair source," OSA Continuum **3**, 1398 (2020).
[151] X. Shi, K. Guo, J. B. Christensen, M. A. Castaneda, X. Liu, H. Ou, and K. Rottwitt, "Multichannel Photon-Pair Generation with Strong and Uniform Spectral Correlation in a Silicon Microring Resonator," Physical Review Applied **12**, 1 (2019).
[152] N. C. Harris, D. Grassani, A. Simbula, M. Pant, M. Galli, T. Baehr-Jones, M. Hochberg, D. Englund, D. Bajoni, and C. Galland, "Integrated source of spectrally filtered correlated photons for large-scale quantum photonic systems," Physical Review X **4**, 41047 (2014).
[153] J. W. Silverstone, R. Santagati, D. Bonneau, M. J. Strain, M. Sorel, J. L. O'Brien, and M. G. Thompson, "Qubit entanglement between ring-

resonator photon-pair sources on a silicon chip," Nature communications **6**, 1–7 (2015).
[154]R. Wakabayashi, M. Fujiwara, K.-i. Yoshino, Y. Nambu, M. Sasaki, and T. Aoki, "Time-bin entangled photon pair generation from Si micro-ring resonator," Optics express **23**, 1103–1113 (2015).
[155]F. Mazeas, M. Traetta, M. Bentivegna, F. Kaiser, D. Aktas, W. Zhang, C. A. Ramos, L. A. Ngah, T. Lunghi, E. Picholle, N. Belabas-Plougonven, X. L. Roux, E. Cassan, D. Marris-Morini, L. Vivien, G. Sauder, L. Labonté, and S. Tanzilli, "High-quality photonic entanglement for wavelength-multiplexed quantum communication based on a silicon chip," Optics express **24**, 28731–28738 (2016).
[156]M. Fujiwara, R. Wakabayashi, M. Sasaki, and M. Takeoka, "Wavelength division multiplexed and double-port pumped time-bin entangled photon pair generation using Si ring resonator," Optics express **25**, 3445–3453 (2017).
[157]C. Ma, X. Wang, V. Anant, A. D. Beyer, M. D. Shaw, and S. Mookherjea, "Silicon photonic entangled photon-pair and heralded single photon generation with CAR> 12,000 and g (2)(0)< 0.006," Optics Express **25**, 32995–33006 (2017).
[158]I. I. Faruque, G. F. Sinclair, D. Bonneau, J. G. Rarity, and M. G. Thompson, "On-chip quantum interference with heralded photons from two independent micro-ring resonator sources in silicon photonics," Optics express **26**, 20379–20395 (2018).
[159]D. Grassani, S. Azzini, M. Liscidini, M. Galli, M. J. Strain, M. Sorel, J. E. Sipe, and D. Bajoni, "Micrometer-scale integrated silicon source of time-energy entangled photons," Optica **2**, 88–94 (2015).
[160]S. F. Preble, M. L. Fanto, J. A. Steidle, C. C. Tison, G. A. Howland, Z. Wang, and P. M. Alsing, "On-chip quantum interference from a single silicon ring-resonator source," Physical Review Applied **4**, 21001 (2015).
[161]D. Grassani, A. Simbula, S. Pirotta, M. Galli, M. Menotti, N. C. Harris, T. Baehr-Jones, M. Hochberg, C. Galland, M. Liscidini, and D. Bajoni, "Energy correlations of photon pairs generated by a silicon microring resonator probed by Stimulated Four Wave Mixing," Scientific reports **6**, 23564 (2016).
[162]M. Davanco, J. R. Ong, A. B. Shehata, A. Tosi, I. Agha, S. Assefa, F. Xia, W. M. J. Green, S. Mookherjea, and K. Srinivasan, "Telecommunications-band heralded single photons from a silicon nanophotonic chip," Applied Physics Letters **100**, 261104 (2012).
[163]S. Azzini, D. Grassani, M. Galli, D. Gerace, M. Patrini, M. Liscidini, P. Velha, and D. Bajoni, "Stimulated and spontaneous four-wave mixing in silicon-on-insulator coupled photonic wire nano-cavities," Applied Physics Letters **103**, 31117 (2013).
[164]N. Matsuda, H. Takesue, K. Shimizu, Y. Tokura, E. Kuramochi, and M. Notomi, "Slow light enhanced correlated photon pair generation in photonic-crystal coupled-resonator optical waveguides," Optics express **21**, 8596–8604 (2013).
[165]C. Xiong, C. Monat, A. S. Clark, C. Grillet, G. D. Marshall, M. J. Steel, J. Li, L. O'Faolain, T. F. Krauss, J. G. Rarity, and B. J. Eggleton, "Slow-light enhanced correlated photon pair generation in a silicon photonic crystal waveguide," Optics letters **36**, 3413–3415 (2011).
[166]R. Kumar, J. R. Ong, J. Recchio, K. Srinivasan, and S. Mookherjea, "Spectrally multiplexed and tunable-wavelength photon pairs at 1.55 μm from a silicon coupled-resonator optical waveguide," Optics letters **38**, 2969–2971 (2013).
[167]J. He, A. S. Clark, M. J. Collins, J. Li, T. F. Krauss, B. J. Eggleton, and C. Xiong, "Degenerate photon-pair generation in an ultracompact silicon photonic crystal waveguide," Optics letters **39**, 3575–3578 (2014).
[168]H. Takesue, N. Matsuda, E. Kuramochi, and M. Notomi, "Entangled photons from on-chip slow light," Scientific reports **4**, 3913 (2014).
[169]J. W. Choi, B.-U. Sohn, G. F. R. Chen, D. K. T. Ng, and D. T. H. Tan, "Correlated photon pair generation in ultra-silicon-rich nitride waveguide," Optics Communications **463**, 125351 (2020).
[170]X. Zhang, Y. Zhang, C. Xiong, and B. J. Eggleton, "Correlated photon pair generation in low-loss double-stripe silicon nitride waveguides," Journal of Optics **18**, 74016 (2016).
[171]F. Samara, A. Martin, C. Autebert, M. Karpov, T. J. Kippenberg, H. Zbinden, and R. Thew, "High-rate photon pairs and sequential Time-Bin entanglement with Si 3 N 4 microring resonators," Optics express **27**, 19309–19318 (2019).
[172]P. Imany, J. A. Jaramillo-Villegas, O. D. Odele, K. Han, D. E. Leaird, J. M. Lukens, P. Lougovski, M. Qi, and A. M. Weiner, "50-GHz-spaced comb of high-dimensional frequency-bin entangled photons from an on-chip silicon nitride microresonator," Optics express **26**, 1825–1840 (2018).
[173]J. A. Jaramillo-Villegas, P. Imany, O. D. Odele, D. E. Leaird, Z.-Y. Ou, M. Qi, and A. M. Weiner, "Persistent energy–time entanglement covering multiple resonances of an on-chip biphoton frequency comb," Optica **4**, 655–658 (2017).
[174]X. Lu, Q. Li, D. A. Westly, G. Moille, A. Singh, V. Anant, and K. Srinivasan, "Chip-integrated visible–telecom entangled photon pair source for quantum communication," Nature physics **15**, 373–381 (2019).
[175]S. Tanzilli, W. Tittel, H. De Riedmatten, H. Zbinden, P. Baldi, M. DeMicheli, D. B. Ostrowsky, and N. Gisin, "PPLN waveguide for quantum communication," The European Physical Journal D-Atomic, Molecular, Optical and Plasma Physics **18**, 155–160 (2002).
[176]O. Alibart, D. B. Ostrowsky, P. Baldi, and S. Tanzilli, "High-performance guided-wave asynchronous heralded single-photon source," Optics letters **30**, 1539–1541 (2005).
[177]F. Setzpfandt, A. S. Solntsev, J. Titchener, C. W. Wu, C. Xiong, R. Schiek, T. Pertsch, D. N. Neshev, and A. A. Sukhorukov, "Tunable generation of entangled photons in a nonlinear directional coupler," Laser & Photonics Reviews **10**, 131–136 (2016).
[178]A. Martin, A. Issautier, H. Herrmann, W. Sohler, D. B. Ostrowsky, O. Alibart, and S. Tanzilli, "A polarization entangled photon-pair source based on a type-II PPLN waveguide emitting at a telecom wavelength," New Journal of Physics **12**, 103005 (2010).
[179]C. Schaeff, R. Polster, R. Lapkiewicz, R. Fickler, S. Ramelow, and A. Zeilinger, "Scalable fiber integrated source for higher-dimensional path-entangled photonic quNits," Optics Express **20**, 16145–16153 (2012).
[180]H. Takesue, K. Inoue, O. Tadanaga, Y. Nishida, and M. Asobe, "Generation of pulsed polarization-entangled photon pairs in a 1.55-μm band with a periodically poled lithium niobate waveguide and an orthogonal polarization delay circuit," Optics letters **30**, 293–295 (2005).
[181]M. Hunault, H. Takesue, O. Tadanaga, Y. Nishida, and M. Asobe, "Generation of time-bin entangled photon pairs by cascaded second-order nonlinearity in a single periodically poled LiNbO 3 waveguide," Optics letters **35**, 1239–1241 (2010).
[182]R. Kruse, L. Sansoni, S. Brauner, R. Ricken, C. S. Hamilton, I. Jex, and C. Silberhorn, "Dual-path source engineering in integrated quantum optics," Physical Review A **92**, 53841 (2015).
[183]H. Jin, F. M. Liu, P. Xu, J. L. Xia, M. L. Zhong, Y. Yuan, J. W. Zhou, Y. X. Gong, W. Wang, and S. N. Zhu, "On-chip generation and manipulation of entangled photons based on reconfigurable lithium-niobate waveguide circuits," Physical review letters **113**, 103601 (2014).
[184]L. Sansoni, K. H. Luo, C. Eigner, R. Ricken, V. Quiring, H. Herrmann, and C. Silberhorn, "A two-channel, spectrally degenerate polarization entangled source on chip," npj Quantum Information **3**, 1–5 (2017).
[185]Y. M. Sua, H. Fan, A. Shahverdi, J.-Y. Chen, and Y.-P. Huang, "Direct generation and detection of quantum correlated photons with 3.2 um wavelength spacing," Scientific reports **7**, 1–10 (2017).
[186]P. Vergyris, T. Meany, T. Lunghi, G. Sauder, J. Downes, M. J. Steel, M. J. Withford, O. Alibart, and S. Tanzilli, "On-chip generation of heralded photon-number states," Scientific reports **6**, 35975 (2016).
[187]R. Ikuta, R. Tani, M. Ishizaki, S. Miki, M. Yabuno, H. Terai, N. Imoto, and T. Yamamoto, "Frequency-Multiplexed Photon Pairs over 1000 Modes from a Quadratic Nonlinear Optical Waveguide Resonator with a Singly Resonant Configuration," Physical Review Letters **123**, 193603 (2019).
[188]E. Pomarico, B. Sanguinetti, N. Gisin, R. Thew, H. Zbinden, G. Schreiber, A. Thomas, and W. Sohler, "Waveguide-based {OPO} source of entangled photon pairs," New Journal of Physics **11**, 113042 (2009).
[189]E. Pomarico, B. Sanguinetti, C. I. Osorio, H. Herrmann, and R. T. Thew, "Engineering integrated pure narrow-band photon sources," New Journal of Physics **14**, 33008 (2012).
[190]J. Zhao, C. Ma, M. Rüsing, and S. Mookherjea, "High quality entangled photon pair generation in periodically poled thin-film lithium niobate waveguides," Phys. Rev. Lett. **124**, 163603 (2020).
[191]A. Yoshizawa, R. Kaji, and H. Tsuchida, "Generation of polarisation-entangled photon pairs at 1550 nm using two PPLN waveguides," Electronics Letters **39**, 621–622 (2003).

[192]H. Chen, S. Auchter, M. Prilmüller, A. Schlager, T. Kauten, K. Laiho, B. Pressl, H. Suchomel, M. Kamp, S. Höfling, and C. Schneider, "Invited Article: Time-bin entangled photon pairs from Bragg-reflection waveguides," APL Photonics **3**, 80804 (2018).
[193]J. Belhassen, F. Baboux, Q. Yao, M. Amanti, I. Favero, A. Lemaître, W. S. Kolthammer, I. A. Walmsley, and S. Ducci, "On-chip III-V monolithic integration of heralded single photon sources and beamsplitters," Applied Physics Letters **112**, 71105 (2018).
[194]R. Horn, P. Abolghasem, B. J. Bijlani, D. Kang, A. S. Helmy, and G. Weihs, "Monolithic source of photon pairs," Physical review letters **108**, 153605 (2012).
[195]P. Sarrafi, E. Y. Zhu, B. M. Holmes, D. C. Hutchings, S. Aitchison, and L. Qian, "High-visibility two-photon interference of frequency–time entangled photons generated in a quasi-phase-matched AlGaAs waveguide," Optics letters **39**, 5188–5191 (2014).
[196]C. Autebert, N. Bruno, A. Martin, A. Lemaitre, C. G. Carbonell, I. Favero, G. Leo, H. Zbinden, and S. Ducci, "Integrated AlGaAs source of highly indistinguishable and energy-time entangled photons," Optica **3**, 143–146 (2016).
[197]C. Autebert, G. Boucher, F. Boitier, A. Eckstein, I. Favero, G. Leo, and S. Ducci, "Photon pair sources in AlGaAs: from electrical injection to quantum state engineering," Journal of Modern Optics **62**, 1739–1745 (2015).
[198]R. T. Horn, P. Kolenderski, D. Kang, P. Abolghasem, C. Scarcella, A. Della Frera, A. Tosi, L. G. Helt, S. V. Zhukovsky, J. E. Sipe, G. Weihs, A. S. Helmy, and T. Jennewein, "Inherent polarization entanglement generated from a monolithic semiconductor chip," Scientific reports **3**, 2314 (2013).
[199]D. Kang, M. Kim, H. He, and A. S. Helmy, "Two polarization-entangled sources from the same semiconductor chip," Physical Review A **92**, 013821 (2015).
[200]A. Vallés, M. Hendrych, J. Svozilík, R. Machulka, P. Abolghasem, D. Kang, B. J. Bijlani, A. S. Helmy, and J. P. Torres, "Generation of polarization-entangled photon pairs in a bragg reflection waveguide," Opt. Express **21**, 10841–10849 (2013).
[201]S. V. Zhukovsky, L. G. Helt, D. Kang, P. Abolghasem, A. S. Helmy, and J. Sipe, "Generation of maximally-polarization-entangled photons on a chip," Physical Review A **85**, 013838 (2012).
[202]P. Kultavewuti, E. Y. Zhu, L. Qian, V. Pusino, M. Sorel, and J. S. Aitchison, "Correlated photon pair generation in AlGaAs nanowaveguides via spontaneous four-wave mixing," Optics express **24**, 3365–3376 (2016).
[203]R. R. Kumar, M. Raevskaia, V. Pogoretskii, Y. Jiao, and H. K. Tsang, "Entangled photon pair generation from an InP membrane micro-ring resonator," Applied Physics Letters **114** (2019), 10.1063/1.5080397.
[204]C. Reimer, M. Kues, P. Roztocki, B. Wetzel, F. Grazioso, B. E. Little, S. T. Chu, T. Johnston, Y. Bromberg, L. Caspani, D. J. Moss, and R. Morandotti, "Generation of multiphoton entangled quantum states by means of integrated frequency combs," Science **351**, 1176–1180 (2016).
[205]M. Kues, C. Reimer, P. Roztocki, L. R. Cortés, S. Sciara, B. Wetzel, Y. Zhang, A. Cino, S. T. Chu, B. E. Little, D. J. Moss, L. Caspani, J. Azaña, and R. Morandotti, "On-chip generation of high-dimensional entangled quantum states and their coherent control," Nature **546**, 622–626 (2017).
[206]C. Reimer, M. Kues, L. Caspani, B. Wetzel, P. Roztocki, M. Clerici, Y. Jestin, M. Ferrera, M. Peccianti, A. Pasquazi, B. E. Little, S. T. Chu, D. J. Moss, and R. Morandotti, "Cross-polarized photon-pair generation and bi-chromatically pumped optical parametric oscillation on a chip," Nature communications **6**, 1–7 (2015).
[207]C. Reimer, L. Caspani, M. Clerici, M. Ferrera, M. Kues, M. Peccianti, A. Pasquazi, L. Razzari, B. E. Little, S. T. Chu, D. J. Moss, and R. Morandotti, "Integrated frequency comb source of heralded single photons," Optics express **22**, 6535–6546 (2014).
[208]C. Xiong, L. G. Helt, A. C. Judge, G. D. Marshall, M. J. Steel, J. E. Sipe, and B. J. Eggleton, "Quantum-correlated photon pair generation in chalcogenide As 2 S 3 waveguides," Optics express **18**, 16206–16216 (2010).
[209]J. B. Spring, P. L. Mennea, B. J. Metcalf, P. C. Humphreys, J. C. Gates, H. L. Rogers, C. Söller, B. J. Smith, W. S. Kolthammer, P. G. R. Smith, and I. A. Walmsley, "Chip-based array of near-identical, pure, heralded single-photon sources," Optica **4**, 90–96 (2017).
[210]S. Clemmen, A. Perret, S. K. Selvaraja, W. Bogaerts, D. Van Thourhout, R. Baets, P. Emplit, and S. Massar, "Generation of correlated photons in hydrogenated amorphous-silicon waveguides," Optics letters **35**, 3483–3485 (2010).
[211]E. Hemsley, D. Bonneau, J. Pelc, R. Beausoleil, J. L. O'Brien, and M. G. Thompson, "Photon pair generation in hydrogenated amorphous silicon microring resonators," Scientific reports **6**, 38908 (2016).
[212]J. Chen, X. Li, and P. Kumar, "Two-photon-state generation via four-wave mixing in optical fibers," Physical Review A **72**, 33801 (2005).
[213]P. Russell, "Photonic crystal fibers," science **299**, 358–362 (2003).
[214]D. Cruz-Delgado, R. Ramirez-Alarcon, E. Ortiz-Ricardo, J. Monroy-Ruz, F. Dominguez-Serna, H. Cruz-Ramirez, K. Garay-Palmett, and A. B. U'Ren, "Fiber-based photon-pair source capable of hybrid entanglement in frequency and transverse mode, controllably scalable to higher dimensions," Scientific Reports **6**, 27377 (2016).
[215]C. Guo, J. Su, Z. Zhang, L. Cui, and X. Li, "Generation of quantum correlated photons in different spatial modes using few-mode fibers," Optics InfoBase Conference Papers **Part F115-LS 2018** (2018), 10.1364/LS.2018.LM1B.8.
[216]Y. Zhang, R. Spiniolas, K. Shinbrough, B. Fang, O. Cohen, and V. O. Lorenz, "Dual-pump approach to photon-pair generation: demonstration of enhanced characterization and engineering capabilities," Optics Express **27**, 19050 (2019).
[217]B. Fang, O. Cohen, J. B. Moreno, and V. O. Lorenz, "State engineering of photon pairs produced through dual-pump spontaneous four-wave mixing," Opt. Express **21**, 2707–2717 (2013).
[218]P. G. Kazansky, P. S. J. Russell, and H. Takebe, "Glass fibre poling and applications," Journal of Lightwave Technology **15**, 1484–1493 (1997).
[219]G. P. Agrawal, Applications of nonlinear fiber optics (Elsevier, 2001).
[220]Y. M. Sua, J. Malowicki, M. Hirano, and K. F. Lee, "Generation of high-purity entangled photon pair in a short highly nonlinear fiber," Optics letters **38**, 73–75 (2013).
[221]Q. Zhou, W. Zhang, J. rong Cheng, Y. dong Huang, and J. de Peng, "Noise performance comparison of 1.5 μm correlated photon pair generation in different fibers," Optics express **18**, 17114–17123 (2010).
[222]Q. Lin and G. P. Agrawal, "Silicon waveguides for creating quantum-correlated photon pairs," Optics letters **31**, 3140–3142 (2006).
[223]P. Sarrafi, E. Y. Zhu, K. Dolgaleva, B. M. Holmes, D. C. Hutchings, J. S. Aitchison, and L. Qian, "Continuous-wave quasi-phase-matched waveguide correlated photon pair source on a iii–v chip," Applied Physics Letters **103**, 251115 (2013).
[224]A. W. Elshaari, I. E. Zadeh, A. Fognini, M. E. Reimer, D. Dalacu, P. J. Poole, V. Zwiller, and K. D. Jöns, "On-chip single photon filtering and multiplexing in hybrid quantum photonic circuits," Nature communications **8**, 1–8 (2017).
[225]W. Bogaerts, P. De Heyn, T. Van Vaerenbergh, K. De Vos, S. Kumar Selvaraja, T. Claes, P. Dumon, P. Bienstman, D. Van Thourhout, and R. Baets, "Silicon microring resonators," Laser & Photonics Reviews **6**, 47–73 (2012).
[226]T. J. Kippenberg, R. Holzwarth, and S. A. Diddams, "Microresonator-based optical frequency combs," science **332**, 555–559 (2011).
[227]N. Matsuda, T. Kato, K.-i. Harada, H. Takesue, E. Kuramochi, H. Taniyama, and M. Notomi, "Slow light enhanced optical nonlinearity in a silicon photonic crystal coupled-resonator optical waveguide," Optics express **19**, 19861–19874 (2011).
[228]S. Saravi, T. Pertsch, and F. Setzpfandt, "Generation of Counterpropagating Path-Entangled Photon Pairs in a Single Periodic Waveguide," Physical Review Letters **118**, 1–6 (2017).
[229]R. Kumar, J. R. Ong, J. Recchio, K. Srinivasan, and S. Mookherjea, "Spectrally multiplexed and tunable-wavelength photon pairs at 1.55μm from a silicon coupled-resonator optical waveguide," Optics Letters **38**, 2969 (2013).
[230]C. Errando-Herranz, E. Schöll, M. Laini, S. Gyger, A. W. Elshaari, A. Branny, U. Wennberg, S. Barbat, T. Renaud, M. Brotons-Gisbert, , C. Bonato, B. D. Gerardot, V. Zwiller, and K. D. Jöns, "On-chip single photon emission from a waveguide-coupled two-dimensional semiconductor," arXiv preprint arXiv:2002.07657 (2020).
[231]F. Lenzini, N. Gruhler, N. Walter, and W. H. P. Pernice, "Diamond as a platform for integrated quantum photonics," Advanced Quantum Technologies **1**, 1800061 (2018).
[232]V. Bharadwaj, O. Jedrkiewicz, J. P. Hadden, B. Sotillo, M. R. Vázquez, P. Dentella, T. T. Fernandez, A. Chiappini, A. N. Giakoumaki, T. L. Phu, M. Bollani, M. Ferrari, R. Ramponi, P. E. Barclay, and S. M. Eaton, "Fem-

tosecond laser written photonic and microfluidic circuits in diamond," Journal of Physics: Photonics **1**, 022001 (2019).
[233]B. J. M. Hausmann, I. Bulu, V. Venkataraman, P. Deotare, and M. Lončar, "Diamond nonlinear photonics," Nature Photonics **8**, 369–374 (2014).
[234]V. Bharadwaj, Y. Wang, T. T. Fernandez, R. Ramponi, S. M. Eaton, and G. Galzerano, "Femtosecond laser written diamond waveguides: A step towards integrated photonics in the far infrared," Optical Materials **85**, 183–185 (2018).
[235]C. Okoth, A. Cavanna, T. Santiago-Cruz, and M. V. Chekhova, "Microscale generation of entangled photons without momentum conservation," Phys. Rev. Lett. **123**, 263602 (2019).
[236]I. Chung and M. G. Kanatzidis, "Metal chalcogenides: a rich source of nonlinear optical materials," Chemistry of Materials **26**, 849–869 (2014).
[237]K. F. Lee, Y. Tian, H. Yang, K. Mustonen, A. Martinez, Q. Dai, E. I. Kauppinen, J. Malowicki, P. Kumar, and Z. Sun, "Photon-pair generation with a 100 nm thick carbon nanotube film," Advanced Materials **29**, 1605978 (2017).
[238]H. Mäntynen, N. Anttu, Z. Sun, and H. Lipsanen, "Single-photon sources with quantum dots in iii–v nanowires," Nanophotonics **8**, 747–769 (2019).
[239]A. Autere, H. Jussila, Y. Dai, Y. Wang, H. Lipsanen, and Z. Sun, "Nonlinear optics with 2d layered materials," Advanced Materials **30**, 1705963 (2018).
[240]H. D. Saleh, S. Vezzoli, L. Caspani, A. Branny, S. Kumar, B. D. Gerardot, and D. Faccio, "Towards spontaneous parametric down conversion from monolayer mos 2," Scientific reports **8**, 1–7 (2018).
[241]L. Marini, L. Helt, Y. Lu, B. J. Eggleton, and S. Palomba, "Constraints on downconversion in atomically thick films," JOSA B **35**, 672–679 (2018).
[242]Y. Wang, M. Ghotbi, S. Das, Y. Dai, S. Li, X. Hu, X. Gan, J. Zhao, and Z. Sun, "Difference frequency generation in monolayer mos2," Nanoscale (2020).
[243]Y. Dai, Y. Wang, S. Das, H. Xue, X. Bai, E. Hulkko, G. Zhang, X. Yang, Q. Dai, and Z. Sun, "Electrical control of interband resonant nonlinear optics in monolayer mos2," ACS nano **14**, 8442–8448 (2020).
[244]Y. Zhang, J. Wu, Y. Yang, Y. Qu, L. Jia, T. Moein, B. Jia, and D. J. Moss, "Enhanced nonlinear optical figure-of-merit at 1550nm for silicon nanowires integrated with graphene oxide layered films," arXiv preprint arXiv:2004.08043 (2020).
[245]A. Ishizawa, R. Kou, T. Goto, T. Tsuchizawa, N. Matsuda, K. Hitachi, T. Nishikawa, K. Yamada, T. Sogawa, and H. Gotoh, "Optical nonlinearity enhancement with graphene-decorated silicon waveguides," Scientific Reports **7**, 45520 (2017).
[246]Q. Feng, H. Cong, B. Zhang, W. Wei, Y. Liang, S. Fang, T. Wang, and J. Zhang, "Enhanced optical Kerr nonlinearity of graphene/Si hybrid waveguide," Applied Physics Letters **114**, 71104 (2019).
[247]N. Vermeulen, D. Castelló-Lurbe, M. Khoder, I. Pasternak, A. Krajewska, T. Ciuk, W. Strupinski, J. Cheng, H. Thienpont, and J. Van Erps, "Graphene's nonlinear-optical physics revealed through exponentially growing self-phase modulation," Nature Communications **9**, 2675 (2018).
[248]K. Chen, X. Zhou, X. Cheng, R. Qiao, Y. Cheng, C. Liu, Y. Xie, W. Yu, F. Yao, Z. Sun, F. Wang, K. Liu, and L. Zhongfan, "Graphene photonic crystal fibre with strong and tunable light–matter interaction," Nature Photonics **13**, 754–759 (2019).
[249]Y. Zuo, W. Yu, C. Liu, X. Cheng, R. Qiao, J. Liang, X. Zhou, J. Wang, M. Wu, Y. Zhao, P. Gao, S. Wu, Z. Sun, K. Liu, X. Bai, and Z. Liu, "Optical fibres with embedded two-dimensional materials for ultrahigh nonlinearity," Nature Nanotechnology , 1–5 (2020).
[250]Y. Yonezu, R. Kou, H. Nishi, T. Tsuchizawa, K. Yamada, T. Aoki, A. Ishizawa, and N. Matsuda, "Evaluation of graphene optical nonlinearity with photon-pair generation in graphene-on-silicon waveguides," Opt. Express **27**, 30262–30271 (2019).
[251]Z. Sun, A. Martinez, and F. Wang, "Optical modulators with 2D layered materials," Nature Photonics **10**, 227–238 (2016).
[252]M. Long, P. Wang, H. Fang, and W. Hu, "Progress, Challenges, and Opportunities for 2D Material Based Photodetectors," Advanced Functional Materials **29**, 1803807 (2019).
[253]D. Armani, T. Kippenberg, S. Spillane, and K. Vahala, "Ultra-high-q toroid microcavity on a chip," Nature **421**, 925–928 (2003).
[254]J. Fürst, D. Strekalov, D. Elser, A. Aiello, U. L. Andersen, C. Marquardt, and G. Leuchs, "Quantum light from a whispering-gallery-mode disk resonator," Physical Review Letters **106**, 113901 (2011).
[255]M. Förtsch, G. Schunk, J. U. Fürst, D. Strekalov, T. Gerrits, M. J. Stevens, F. Sedlmeir, H. G. L. Schwefel, S. W. Nam, G. Leuchs, and C. Marquardt, "Highly efficient generation of single-mode photon pairs from a crystalline whispering-gallery-mode resonator source," Physical Review A **91**, 23812 (2015).
[256]E. Pomaríco, B. Sangulnettl, N. Gisin, R. Thew, H. Zbinden, G. Schreiber, A. Thomas, and W. Sohler, "Waveguide-based OPO source of entangled photon pairs," New Journal of Physics **11** (2009), 10.1088/1367-2630/11/11/113042, arXiv:0909.1208.
[257]E. Pomarico, B. Sanguinetti, C. I. Osorio, H. Herrmann, and R. T. Thew, "Engineering integrated pure narrow-band photon sources," New Journal of Physics **14** (2012), 10.1088/1367-2630/14/3/033008.
[258]L. Li, Z. Liu, X. Ren, S. Wang, V.-C. Su, M.-K. Chen, C. H. Chu, H. Y. Kuo, B. Liu, W. Zang, G. Guo, L. Zhang, Z. Wang, S. Zhu, and D. P. Tsai, "Metalens-array–based high-dimensional and multiphoton quantum source," Science **368**, 1487–1490 (2020), https://science.sciencemag.org/content/368/6498/1487.full.pdf.
[259]A. N. Poddubny, I. V. Iorsh, and A. A. Sukhorukov, "Generation of photon-plasmon quantum states in nonlinear hyperbolic metamaterials," Phys. Rev. Lett. **117**, 123901 (2016).
[260]M. S. Tame, K. McEnery, Ş. Özdemir, J. Lee, S. A. Maier, and M. Kim, "Quantum plasmonics," Nature Physics **9**, 329–340 (2013).
[261]G. Marino, A. S. Solntsev, L. Xu, V. F. Gili, L. Carletti, A. N. Poddubny, M. Rahmani, D. A. Smirnova, H. Chen, A. Lemaître, G. Zhang, A. V. Zayats, C. De Angelis, G. Leo, A. A. Sukhorukov, and D. N. Neshev, "Spontaneous photon-pair generation from a dielectric nanoantenna," Optica **6**, 1416–1422 (2019).
[262]G. Laurent, N. Chauvet, G. Nogues, A. Drezet, and G. Bachelier, "Photon-pair production at the nanoscale with hybrid nonlinear/plasmonic antennas," arXiv preprint arXiv:1806.08702 (2018).
[263]A. Davoyan and H. Atwater, "Quantum nonlinear light emission in metamaterials: broadband purcell enhancement of parametric downconversion," Optica **5**, 608–611 (2018).
[264]M. Müller, S. Bounouar, K. D. Jöns, M. Glässl, and P. Michler, "On-demand generation of indistinguishable polarization-entangled photon pairs," Nature Photonics **8**, 224–228 (2014).
[265]F. Kaneda, B. G. Christensen, J. J. Wong, H. S. Park, K. T. McCusker, and P. G. Kwiat, "Time-multiplexed heralded single-photon source," Optica **2**, 1010–1013 (2015).
[266]C. Xiong, X. Zhang, Z. Liu, M. J. Collins, A. Mahendra, L. G. Helt, M. J. Steel, D.-Y. Choi, C. J. Chae, P. H. W. Leong, and B. J. Eggleton, "Active temporal multiplexing of indistinguishable heralded single photons," Nature communications **7**, 1–6 (2016).
[267]Y.-H. Li, Z.-Y. Zhou, L.-T. Feng, W.-T. Fang, S.-l. Liu, S.-K. Liu, K. Wang, X.-F. Ren, D.-S. Ding, L.-X. Xu, and B.-S. Shi, "On-chip multiplexed multiple entanglement sources in a single silicon nanowire," Physical Review Applied **7**, 64005 (2017).
[268]T. Meany, L. A. Ngah, M. J. Collins, A. S. Clark, R. J. Williams, B. J. Eggleton, M. J. Steel, M. J. Withford, O. Alibart, and S. Tanzilli, "Hybrid photonic circuit for multiplexed heralded single photons," Laser & Photonics Reviews **8**, L42—-L46 (2014).
[269]C. Joshi, A. Farsi, S. Clemmen, S. Ramelow, and A. L. Gaeta, "Frequency multiplexing for quasi-deterministic heralded single-photon sources," Nature Communications **9**, 847 (2018).
[270]T. J. Seok, K. Kwon, J. Henriksson, J. Luo, and M. C. Wu, "240 $\times$ 240 wafer-scale silicon photonic switches," Optical Fiber Communication Conference , Th1E—-5 (2019).
[271]J. Wang, S. Paesani, Y. Ding, R. Santagati, P. Skrzypczyk, A. Salavrakos, J. Tura, R. Augusiak, L. Mančinska, D. Bacco, D. Bonneau, J. W. Silverstone, Q. Gong, A. Acín, K. Rottwitt, L. K. Oxenløwe, J. L. O'Brien, A. Laing, and M. G. Thompson, "Multidimensional quantum entanglement with large-scale integrated optics," Science **360**, 285–291 (2018).
[272]J. F. Bauters, M. J. R. Heck, D. D. John, J. S. Barton, C. M. Bruinink, A. Leinse, R. G. Heideman, D. J. Blumenthal, and J. E. Bowers, "Planar waveguides with less than 0.1 dB/m propagation loss fabricated with wafer bonding," Optics express **19**, 24090–24101 (2011).
[273]Z. Xie, T. Zhong, S. Shrestha, X. Xu, J. Liang, Y.-X. Gong, J. C. Bienfang, A. Restelli, J. H. Shapiro, F. N. Wong, and C. W. Wong, "Harnessing high-dimensional hyperentanglement through a biphoton frequency comb," Na-

ture Photonics **9**, 536–542 (2015).
[274]G. Maltese, M. Amanti, F. Appas, G. Sinnl, A. Lemaitre, P. Milman, F. Baboux, and S. Ducci, "Generation and symmetry control of quantum frequency combs," npj Quantum Information **6**, 1–6 (2020).
[275]M. Kues, C. Reimer, J. M. Lukens, W. J. Munro, A. M. Weiner, D. J. Moss, and R. Morandotti, "Quantum optical microcombs," Nature Photonics **13**, 170–179 (2019).
[276]I. M. Georgescu, S. Ashhab, and F. Nori, "Quantum simulation," Reviews of Modern Physics **86**, 153 (2014).
[277]A. M. Childs, "Universal computation by quantum walk," Physical review letters **102**, 180501 (2009).
[278]M. Tillmann, B. Dakić, R. Heilmann, S. Nolte, A. Szameit, and P. Walther, "Experimental boson sampling," Nature photonics **7**, 540–544 (2013).
[279]J. B. Spring, B. J. Metcalf, P. C. Humphreys, W. S. Kolthammer, X.-M. Jin, M. Barbieri, A. Datta, N. Thomas-Peter, N. K. Langford, D. Kundys, J. C. Gates, B. J. Smith, P. G. R. Smith, and I. A. Walmsley, "Boson sampling on a photonic chip," Science **339**, 798–801 (2013).
[280]H. Wang, J. Qin, X. Ding, M.-C. Chen, S. Chen, X. You, Y.-M. He, X. Jiang, L. You, Z. Wang, C. Schneider, J. J. Renema, S. Höfling, C.-Y. Lu, and J.-W. Pan, "Boson sampling with 20 input photons and a 60-mode interferometer in a 10^{14}-dimensional hilbert space," Phys. Rev. Lett. **123**, 250503 (2019).
[281]E. Knill, R. Laflamme, and G. J. Milburn, "A scheme for efficient quantum computation with linear optics," nature **409**, 46–52 (2001).
[282]K. Chen, C.-M. Li, Q. Zhang, Y.-A. Chen, A. Goebel, S. Chen, A. Mair, and J.-W. Pan, "Experimental realization of one-way quantum computing with two-photon four-qubit cluster states," Phys. Rev. Lett. **99**, 120503 (2007).
[283]P. Walther, K. J. Resch, T. Rudolph, E. Schenck, H. Weinfurter, V. Vedral, M. Aspelmeyer, and A. Zeilinger, "Experimental one-way quantum computing," Nature **434**, 169–176 (2005).